Design of a stable optical system with an injection-locked laser to cool quantum gases to ultracold temperatures

A Dissertation

submitted to the

Indian Institute of Science Education and Research, Pune
in partial fulfillment of the requirements for the
BS-MS Dual Degree Programme

Anwesh Bhattacharya

Indian Institute of Science Education and Research Pune
Dr. Homi Bhabha Road,
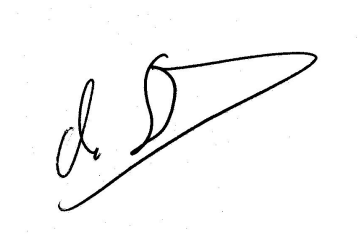Pashan, Pune 411008, INDIA.

01 April, 2019

Supervisor: Prof. Christophe Salomon

© Anwesh Bhattacharya 2019

Certificate

This is to certify that this dissertation, entitled "Design of a stable optical system with an injection-locked laser to cool quantum gases to ultracold temperatures", submitted towards the partial fulfillment of the requirements of the BS-MS dual degree programme at the Indian Institute of Science Education and Research, Pune represents study/work carried out by Anwesh Bhattacharyaat the Laboratoire Kastler Brossel, École Normale Supérieure, Paris under the supervision of Prof. Christophe Salomon, Director of Research at CNRS, Laboratoire Kastler Brossel, École Normale Supérieure, Paris during the academic year 2018-2019.

Prof. Christophe Salomon

Thesis Advisory Committee:

Prof. Christophe Salomon

Prof. Satish Ogale

This thesis is dedicated to KP for challenging me to come this far,
and to Nandz and Mice for believing in my ability to do so.

Declaration

I hereby declare that the matter embodied in the report entitled "Design of a stable optical system with an injection-locked laser to cool quantum gases to ultracold temperatures ", is the result of the work carried out by me at the Laboratoire Kastler Brossel, École Normale Supérieure, Paris, under the supervision of Prof. Christophe Salomon and the same has not been submitted elsewhere for any other degree.

Anwesh Bhattacharya

Acknowledgments
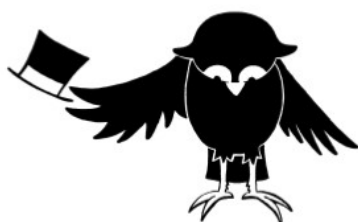
This Master's thesis is the culmination of a five-year long journey at IISER Pune, and I am painfully aware from the outset that it will not be possible to thank each and every one who has helped me in some way or the other, at some point during this journey, in ways which may not even be known to me. I tender my sincere apologies for being unable to do justice to every benefactor of mine, but here's a deeply grateful shout-out to the universe and its constituents for having my back all along!

Firstly, I would like to thank Prof. Christophe Salomon for introducing me to the field of Ultracold atomic gases, and for mentoring me patiently throughout the whole project. His disarming cheer infused in me the strength to carry on with my project, even while living away from Pune, and I have been fortunate to have been guided by such a benevolent physicist. I would also like to express my gratitude to Prof. Tarik Yefsah and Prof. Frederic Chevy for mentoring me through discussions and lab meetings and also for ensuring in making my stay in the group enjoyable. In this project, I would not have been able to do the work I have done without the unstinted support of Gentle and Kunlun, who held my hands and offered every support possible while doing experiments, at the cost of their own busy schedules. I am also grateful to Matthieu, Ragheed and Shuwei for helping me whenever I called upon them for advice. My stay in the Ultracold Fermi Gases group wouldn't have been half as pleasant and joyful if not for the warmth and congeniality of Clement, Cedric, Dr. Tom,

Julian, Yann, Clara, Joanna and Darby. I would also fall short if I fail to appreciate the involved efforts of Thierry, Nora, Stephanie, Celine, Valerie, Philippe, Lionel, Toufik and Denis for helping me out with the many tasks at LKB.

Having left India for the first time in my life, I would not have been able to live as joyfully as I did in Paris without my dear Nandu, who ensured that I had all the freedom from social obligations to peacefully procrastinate and write this thesis. I cannot thank him enough for being my family here, along with everyone who drank *Haldi wala doodh* - Surabhi, Kirti, Sachin, Sagar, Vaibhav and Amar.

My journey at IISER Pune would have been unthinkable without my small family Makuna Hatata - Shubham, Suraj, Shrunal, Shraddha, Aayush, Dimple and Mukul - who were gracious and patient enough to tolerate my craziness for all these years. I am in the debt of friends like Bhaskar, Aanjaneya, Suman and Projjwal who have made sure that I was doing fine in trying times. Life at IISER would have been morose had I not been immersed in theatre, and for which I am eternally in the debt of every single person in the Drama Club, another of my big families who lifted my spirits up in trying times. I would also like to thank Diptabrata, Akash, Priya and Debarshi for teaching me all the undergraduate Physics which I do know, which is extremely minuscule and insufficient, Rajesh Mondal for being my first and possibly the best doctoral mentor in a semester project, members of the Optics lab who made me fall in love with the field, and all the different clubs in IISER Pune which kept me alive through my stay.

I have been blessed to have been fed by folks running the Mess, MDC Canteen, Shivsagar, Ankita Enterprises, to have been given much leeway in classes by the attendance personnel at LHC, to have been always entertained jovially in the Academic Office (which I call Acads), to have been helped always in the library, and to have been able to dwell in a place as productive as the Bhaskara lab (my room # 227 was the opposite!).

In academics and research, I have been extremely fortunate to have been mentored by such brilliant teachers and researchers as Prof. Satish Ogale, Prof. G. V. Pavan Kumar, Prof. Bhas Bapat, Prof. John Mathew, Prof. Pushkar Sohoni, Prof. Anil Zankar, and all the other splendid faculty members at IISER Pune whose passion for their field infected me in unbeknownst ways. I would be guilty if I did not thank Prof. Anwesh Mazumdar at HBCSE, TIFR, Mumbai who introduced me to research in my first year, and patiently mentored me through my slow progress over three years. I am thankful to him for his kindness and

humour, and also to all the members of the Astronomy Cell which I called home for all of my summer vacations. NIUS at HBCSE wouldn't have been the same without Uddipan and Kshitij to chillax with, and without such beautiful people as Smriti and Pulkit who were always punctual in meeting me and turning my evenings and nights bright and cheery!

I have also been really lucky to have such awesome seniors as my 3rd years and my 2nd year seniors, who did not shy away from helping me always and anytime, even after I had not given a proper "introduction" to anyone of them. I believe that each one of them was instrumental in fostering the conducive culture and atmosphere at IISER Pune, which enabled me to not lose my sanity and survive with my craziness in the academic madness.

Not many people can have the great fortune of having a family after leaving home for the first time to study in a college, but I have been blessed with one in Pune, a place where I could not only go to relish *maach* delicacies when I badly craved them, but to whom I could turn to for anything that made me miss home. I am deeply grateful and lucky to be in the debt of Monima, Bubka, Meso and Didu, who did not make me feel that I was away from my own home, in a city on the other side of the country.

Finally, as all such lists have to end, even though we may not want them to, I come to my turn to speak of those folks for whom I am still poor enough to muster enough gratitude for all they have done for me. Baba has taught me to value education and knowledge above all else, and that has been my guiding star in my undergraduate life at IISER Pune. Ma has showed me how nothing is the world is greater than compassion, and I have strived to be a little bit more so during my life outside home. I will never be able to thank them, but I am sure that if I am given the chance to thank anyone, it would be them. In any case, I am glad that even while I'm in Paris, they have learnt how to use smartphones to video-call me and tease me with the lipsmacking food at home and their fascinating travels across the country. In my life, I would have done everything that I have done, much lesser, if there wasn't an evil spirit to pillow-fight with me and to always keep complaining about me and disturb my peace. If not for Bonu, I would not have known the pain of throwing someone off a bicycle, and the tears of love welling in the eyes after still being trusted for another bike ride. I am not sure why I have been showered with such love in my life from so many people. I hope that in my quest to find the answer to that, I keep living for others, and also prank Bonu in a million ways on April Fools' Day.

I would fall short hither if I did not pay my gratitude to Daanish, for everything she has

done for me, and particularly for ensuring that I could work on my thesis and presentation even when I did not have all the means to do so. My deepest and sincerest affection lies with her!

To all that is joyful in this world, I pay my obeisance!

Abstract

Strongly-correlated fermions are ubiquitous in nature, from the quark-gluon plasma of the early universe to neutron stars found in outer space, they lie at the heart of many modern materials such as high-temperature superconductors, massive magneto-resistance devices and graphene, and present some of the most challenging problems in contemporary physics. A thorough understanding of strongly correlated fermions will be able to address a wide range of questions from fundamental physics to technological applications. However, such an understanding is often hindered by the complexity of the host systems themselves. In addition, they are very difficult to treat theoretically, either analytically or numerically, due to the exponential increase in complexity even for a fairly small number of interacting particles. On the other hand, ultracold gas experiments have been successful in setting fermions in a well-characterized environment with a broad degree of control over inter-species interactions. In these systems, one can add a single ingredient at a time (spin mixture, interactions, lattice, etc.), allowing for an incremental complexity, which is analoguous to a quantum simulator for directly testing many-body theories. In many cases, the properties of such systems are universal and experimental results can be directly applied to explain the behaviour of natural materials.

In this dissertation, I discuss about my Masters project which is devoted to the design of a stable optical system with an injection-locked laser to cool Lithium gases to ultracold temperatures in order for the Lithium atoms to be manipulated as required for the scientific experiments. The purpose of a stable optical system design is to have a steady time-invariant frequency and intensity control of the laser setup. The laser setup will be then used to cool down Lithium atoms to temperatures on the order of 40 μK by laser cooling. Subsequently, these ultracold Lithium atoms will be manipulated in the compound setup, already developed in our laboratory, to study the behaviour of the Bose and Fermi gases in the unitarity regime between the BEC-BCS crossover. I will summarise the relevant theory required for the design of such a system, and also highlight the experimental work carried out to realize it. The report culminates with a discussion on further work to be done in the future, and its utilization in the global compound apparatus used in the laboratory to study ultracold Bose and Fermi gases.

Contents

List of Figures

Chapter 1

Introduction

1.1 Ultracold Gas Research

Strongly-correlated fermions are ubiquitous in nature, from the quark-gluon plasma of the early universe to neutron stars found in outer space, they lie at the heart of many modern materials such as high-temperature superconductors, massive magneto-resistance devices

and graphene, and present some of the most challenging problems in contemporary physics. A thorough understanding of strongly correlated fermions will be able to address a wide range of questions from fundamental physics to technological applications. However, such an understanding is often hindered by the complexity of the host systems themselves. In addition, they are very difficult to treat theoretically, either analytically or numerically, due to the exponential increase in complexity even for a fairly small number of interacting particles [1].

On the other hand, ultracold gas experiments have been successful in setting fermions in a well-characterized environment with a broad degree of control over inter-species interactions. In these systems, one can add a single ingredient at a time (spin mixture, interactions, lattice, etc.), allowing for an incremental complexity, which is analoguous to a quantum simulator for directly testing many-body theories. In many cases, the properties of such systems are universal and experimental results can be directly applied to explain the behaviour of natural materials.

The immense advantages that are afforded by ultracold gas systems have been utilized by research groups in understanding strongly-correlated quantum systems, and this active field of research is looking at problems in many different directions. Our research group has already done pioneering experiments to realize superfluidity in Bose and Fermi gases. The present purpose of the group is to develop ultracold gas systems with the ability to manipulate single atoms and observe their interaction dynamics.

1.2   Lab Overview

Presently, the Ultracold Fermi Gases research group has 3 laboratories devoted to multiple projects in the broad field of ultracold atoms, primarily using lithium and potassium atoms. I have interacted with members of all the 3 labs, and hereafter follows my brief summary of the ongoing projects being undertaken by the group.

In the old Lithium 1 lab, ^{7}Li - which is a Bose gas with nice Feshbach resonance - and ^{6}Li - which is a Fermi gas with strongly interacting up & down spins - are together seen to show perfect superfluidity at absolute zero temperature, i.e. no viscosity. If the superfluid is forced through a finite aperture at sufficiently high speed, viscosity comes into play leading to a

breakdown of zero temperature superfluidity, and we obtain a finite temperature superfluid which has an ideal superfluid part and excitations arising from quasi-particles. Tan's contact [2][3] is a microscopic property that depends on how a system of two fermions (spin up & spin down) are bound, and it is related to the global parameters of the fermionic gas. In experiments carried out in this lab, Tan's contact was found by measuring the global thermodynamic parameters. A zero temperature Fermi gas has an occupation versus energy graph that resembles a step function. The occupation below k_F is 1 while beyond k_F is 0. In Fermi gases at finite temperature, it is not exactly an ideal step function as some holes reduce the occupation count below k_F and some free fermions increase the occupation count above k_F, with interactions in the Fermi gas further modifying the Fermi surface. Additionally, in a harmonic potential, the edge fermions behave like those in the ideal gas case while the ones at the centre of the trap behave like a strongly interacting gas. It is possible to find a theoretical connection between the microscopic properties of the particles and the global thermodynamic parameters of the atomic gases through the two-body Tan's contact. It relates the probability of having two particles with the same spin in a finite volume to the global parameters of the gas like its rate of change of energy with respect to the scattering length at a fixed entropy. Tan's contact can be defined in two ways, at equilibrium:

$$\lim_{k \to \infty} n(k) \to \frac{C_2}{k^4} \tag{1.1}$$

$$C_2 \equiv \frac{-4\pi m}{\hbar^2} \left\{ \frac{\partial E}{\partial(1/a_F)} \right\}_S \tag{1.2}$$

where the derivative is evaluated with the entropy S held fixed [4].

If two spins are at r_1 & r_2:

$$_{(r_2-r_1)\to 0}C_2 \propto \frac{1}{|r_2 - r_1|^2} \tag{1.3}$$

The zero temperature Tan's contact behaviour has been measured right from BEC to BCS, through unitarity [6]. The physics on either side far off of unitarity is known, but not exactly at unitarity, and the interesting physics regime falls between $-1 < k_F < 1$.

In the new Lithium 3 lab, atoms are being laser cooled to reduce the kinetic energy spread of the atomic cloud. With the capability of single atom resolution, where the atoms are held in place by strong traps, atoms are imaged by Fluorescence Optical Miscroscopy [5].

The atoms are laser cooled during detection to ensure that they stay in resonance during the imaging. [7]

In the Fermix lab, atoms of ^{6}Li & ^{40}K are used to study mixtures of mass-imbalanced fermionic systems. The atoms of both species are put together in a fermionic system, and they can be trapped and manipulated either separately or together. Interesting physics which arises from such systems include the impurity problem, where a single K quantum dot (0D) is placed in a sea of Li atoms (3D) and their interaction is observed. Other geometries like 3D Li bowl on a 2D K plane, either below or intersecting the bowl are also studied.

1.3 Project Objective

The aim of my Masters' project is to design a stable optical system with an injection-locked laser to cool quantum gases to low temperatures. The purpose of a stable optical system design is to have a steady time-invariant frequency and intensity control of the laser setup. The laser setup will be then used to cool down Lithium atoms to temperatures on the order of 1 mK by laser cooling and then to about 40 μK by evaporative cooling, leading to quantum degeneracy of the Fermi gas. Subsequently, these ultracold Lithium atoms will be manipulated in the compound setup, already developed and presently being refurbished in the laboratory, to study the behaviour of the Bose and Fermi gases in the mixed superfluid phases in the unitarity regime between the BEC-BCS crossover [8]. On the BEC side, there is Bose-Einstein condensation of diatomic molecules in the atomic Fermi gas with positive scattering length, while on the BardeenCooperSchrieffer (BCS) side, fermions exist in a state of weakly correlated pairs, with negative scattering length. The crossover from the BEC to the BCS side is the unitary regime, and at the unitary limit, the scattering length goes to zero.

Chapter 2

Theory

For the design of a stable optical setup for laser cooling, it is necessary to know the theory behind the functioning of laser diodes and the physical considerations that need to be assessed before designing an optimum system of laser resonators. I will begin by reviewing the key concepts for designing a good laser resonator[9], followed by a review of the essential considerations for setting up a stable diode laser [11]. I will then discuss about the Lithium atom and its atomic transitions.

2.1 Laser beams and resonators

Laser beams in the optical or infrared wavelength spectrum have a beam diameter significantly larger than the wavelength. The first laser resonators were based on the Fabry-Perot interferometer. We will first look at the paraxial ray analysis of laser beams, a theory based on geometrical optics, followed by a second theory analysing laser beams by taking into account their wave nature but ignoring the effects of diffraction which arise due to a finite aperture, concluding with the final part that incorporates diffraction effects into the wave theory.

2.1.1 Paraxial Ray Analysis

The propagation of paraxial rays through optical structures can be described by ray transfer matrices, which also describe the propagation of Gaussian beams through those structures. A study of the passage of paraxial rays through optical resonators reveals geometrical properties like the stability of resonators, and loss in unstable ones. In the matrix form,

$$\begin{pmatrix} x_2 \\ x_2' \end{pmatrix} = \begin{pmatrix} A & B \\ C & D \end{pmatrix} \begin{pmatrix} x_1 \\ x_1' \end{pmatrix} \tag{2.1}$$

where (ABCD) is the ray transfer matrix (RTM).

In a laser resonator, light rays bounce back and forth between spherical mirrors and undergo periodic focusing similar to a lens sequence, which can be described by a multiplication of the equivalent lens RTMs. The stability criterion is

$$-1 < \frac{1}{2}(A + D) < 1 \tag{2.2}$$

where instability means the dispersal of rays and loss of periodic refocusing.

2.1.2 Wave Analysis

The wave analysis of laser beams is carried out by considering large apertures that intercept only a negligible portion of the beam, and thereby ignoring aperture diffraction effects. The
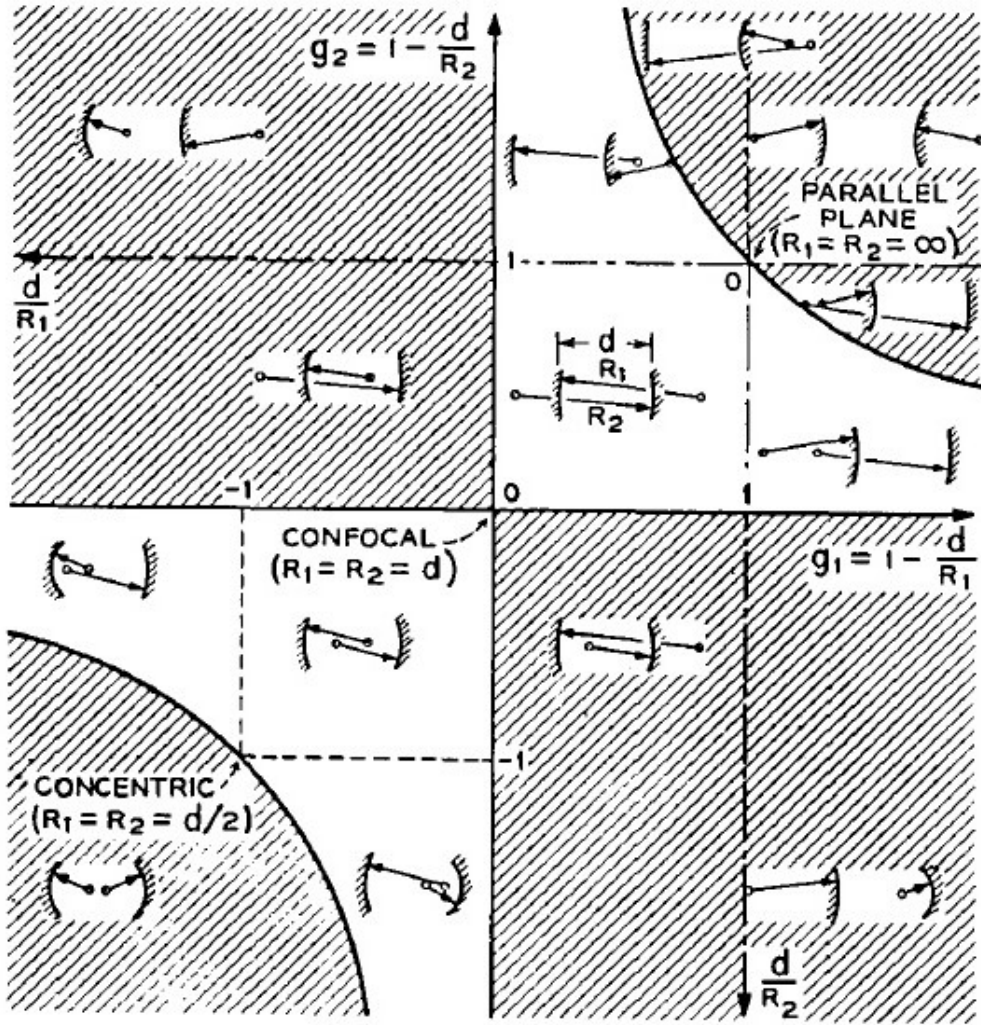
Figure 2.1: Stability diagram of laser resonators, with unstable regions being shaded [9].

intensity distribution of laser beams are concentrated near the axis of propagation, the beam expands with propagation distance and the phase fronts are slightly curved, in contrast to otherwise similar plane waves. By assuming a slowly-varying envelope, the differential wave equation has a solution similar to that of the time-dependent Schrödinger equation:

$$\psi = e^{-j(P + \frac{k}{2q} r^2)} \tag{2.3}$$

Even though there are more solutions, this solution which represents a coherent light beam with a Gaussian intensity profile is very important and is known as the fundamental

mode. The contour of the Gaussian beam is shown:
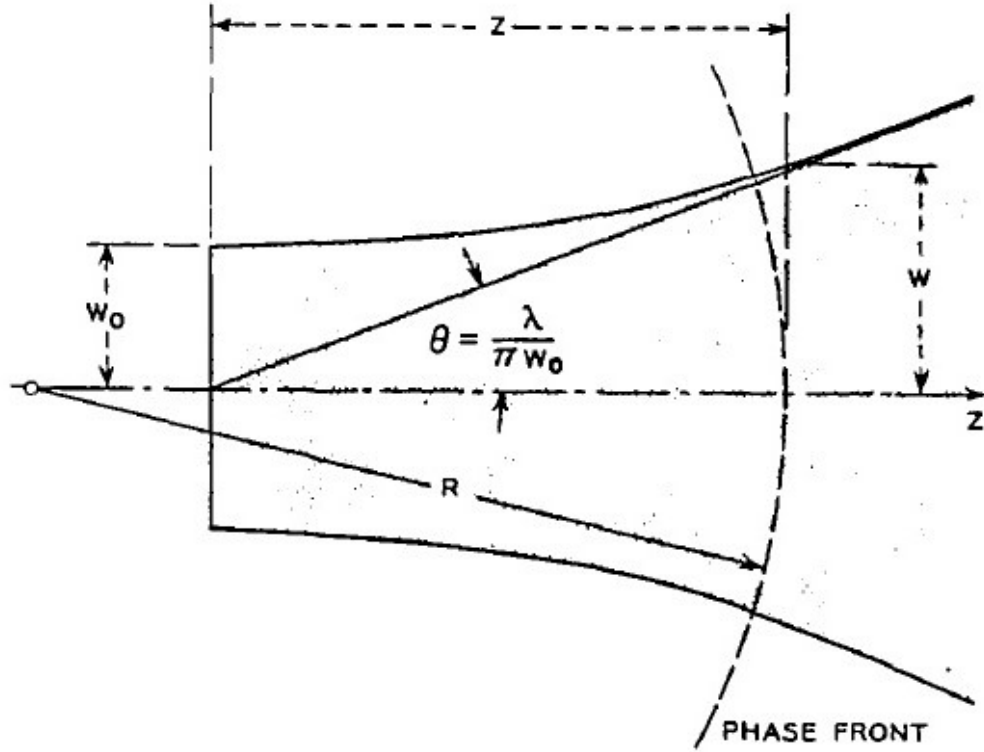
Figure 2.2: Contour of a Gaussian beam [9]

and two very important scaling relations are:

$$w_0^2 = w^2/[1 + (\frac{\pi w^2}{\lambda R})^2]$$ (2.4)

$$z = R/[1 + (\frac{\lambda R}{\pi w^2})^2]$$ (2.5)

The Gaussian beam can be represented by

$$u(r, z) = \frac{w_0}{w}.e^{-j(kz - \Phi) - r^2(\frac{1}{w^2} + \frac{jk}{2R})}$$ (2.6)

The complete and orthogonal set of solutions are called the modes of propagation. In Cartesian coordinates, the intensity profile pattern in higher order beams is described by the product of Hermite and Gaussian functions, while modes in cylindrical coordinates are described by the product of Laguerre & Gaussian polynomials. The parameter R(z), related to the curvature of the phase-front is the same for all modes, while the phase shift is a function

10

of the mode number, with phase velocity being directly proportional to mode number. These lead to different resonator frequencies for the various oscillation modes.

Lenses can be used to focus or produce laser beams with suitable diameters and phase-front curvatures. An ideal lens system keeps the mode intact while changing the R(z) - the radius of curvature of the wavefront upon intersection at the axis - and w(z), a measure of the amplitude decrease away from the axis, transforming the wavefronts of laser beams in exactly the same way as those of spherical waves. The q-parameters of the incoming and outgoing beams are related by the thin lens formula, and according to the figure below
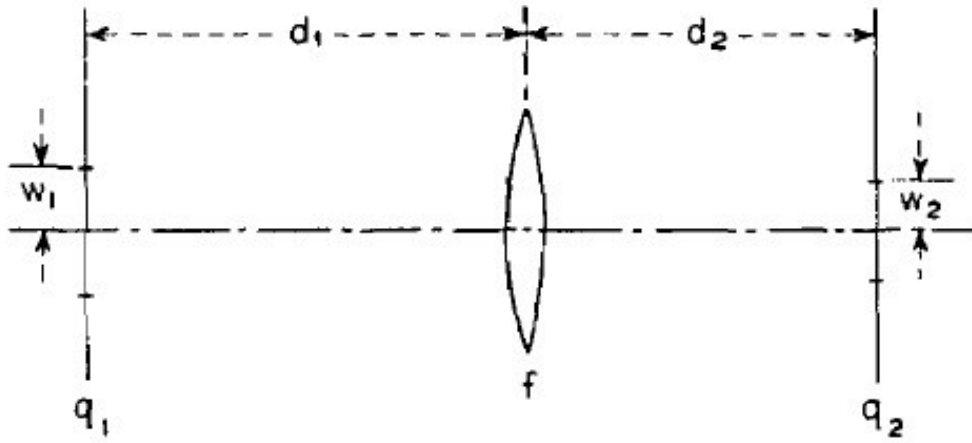
Figure 2.3: Distances and parameters for a beam transformed by a thin lens [9]

can be calculated by

$$q_2 = \frac{(1 - d_2/f)q_1 + (d_1 + d_2 - d_1d_2/f)}{-(q_1/f) + (1 - d_1/f)} \qquad (2.7)$$

or, if the ray transfer matrix is known, by the ABCD law, which follows from the analogous nature between spherical waves in geometrical optics and laser beams:

$$q_2 = \frac{Aq_1 + B}{Cq_1 + D} \qquad (2.8)$$

Stable laser resonators are studied, taking into account the wave nature of the laser beams, in the infinite aperture approximation i.e. when the spot size is significantly less than the aperture. A resonator mode between two spherical mirrors in a laser resonator

11

forms an axial standing-wave pattern, and the beam parameters follow a self-consistency criterion after a complete return trip of the beam. It can be shown that the mirror surfaces are coincident with the phase fronts of the resonator modes. The width of the fundamental mode is

$$w^2 = \frac{\lambda R}{\pi} \Big/ \sqrt{2\frac{R}{d} - 1} \tag{2.9}$$

The resonant frequency of a mode is

$$\nu/\nu_0 = (q+1) + \frac{1}{\pi}(m+n+1)\,cos^{-1}(1 - d/R) \tag{2.10}$$

for rectangular modes, and the (m+n+1) term is replaced by (2p+l+1) for modes with circular geometry.

In many cases, output beams from laser resonators are injected into optical structures with different beam parameters. In such cases, beam transformation using a thin lens (or more complex systems) is necessary to match the modes of one structure to those of another. The locations of the waists of the two beams and their corresponding beam diameters are usually known. One has to choose an appropriate lens with a focal length larger than the characteristic length

$$f_0 = \pi w_1 w_2 / \lambda \tag{2.11}$$

to transform the beam. After f is chosen, the distances d_1 & d_2 have to be adjusted according to:

$$d_1 = f \pm \frac{w_1}{w_2}\sqrt{f^2 - f_0^2} \tag{2.12}$$

$$d_2 = f \pm \frac{w_2}{w_1}\sqrt{f^2 - f_0^2} \tag{2.13}$$

as can be seen from Fig. 2.3. It is helpful to know the accuracy of distance adjustments during the design of a matching system. Using the confocal parameters

$$b_1 = 2\pi w_1^2 / \lambda \tag{2.14}$$

$$b_2 = 2\pi w_2^2 / \lambda \tag{2.15}$$

if b_1 & f are fixed, b_2 of the output beam changes with d_1 according to a Lorentzian functional form centred at $d_1 = f$ with a width of b_1, and the value of $b_2 \leq (4f^2)/b_1$. d_2 changes with

d_1 according to

$$1 - d_2/f = \frac{1 - d_1/f}{(1 - d_1/f)^2 + (b_1/2f)^2} \tag{2.16}$$

2.1.3   Laser Resonators (Finite Aperture)

Laser resonators with finite mirror apertures are intrinsically lossy due to diffraction losses, and the electromagnetic field inside decays slowly if there is no continuous supply of energy. The relative distribution of these modes, however, are time-invariant. In laser oscillators, a steady-state field exists as the active medium supplies adequate energy to overcome the losses. However, due to non-linear gain saturation, there is lower gain in regions with higher field; recent results show that saturation effects are non-perturbative if the gain is not too high. By assuming the quasi-optic nature of the open resonator, specifically two conditions: 1. that the wavelength is substantially lesser than the resonator dimensions, and 2. that the field in the resonator is mostly transverse electromagnetic, the Fresnel-Kirchhoff formulation of Huygens principle can be invoked to arrive at two integral equations:

$$\gamma^{(1)} E^{(1)}(s_1) = \int_{S_2} K^{(2)}(s_1, s_2) E^{(2)}(s_2) dS_2 \tag{2.17}$$

$$\gamma^{(2)} E^{(2)}(s_2) = \int_{S_1} K^{(1)}(s_2, s_1) E^{(1)}(s_1) dS_1 \tag{2.18}$$

relating the fields of the opposite mirrors. If the mirror separation is larger than the mirror dimensions, with only slight mirror curvature, the two orthogonal Cartesian vector field components are uncoupled whose solution yields resonator modes with uniform polarization in a single direction, linear superposition of which can be used to obtain other configurations.

For spherical mirrors, with rectangular or circular apertures , the 2-D integral equations are separable and reduce to 1-D equations whose solutions are tractable. Exact analytical solutions have been found only for the special case of confocal resonators, but many others can be solved numerically. The calculations for obtaining solutions for different resonators is reduced by three equivalence conditions. Interchanging mirrors, reversal of sign of g_1 & g_2, defined below:

$$g_1 = 1 - \frac{d}{R_1} \tag{2.19}$$

$$g_2 = 1 - \frac{d}{R_2} \tag{2.20}$$

and the equality of all the three - Fresnel number N and stability factors G_1 & G_2, defined below:

$$N = \frac{a_1 a_2}{\lambda d} \tag{2.21}$$

$$G_1 = g_1 \frac{a_1}{a_2} \tag{2.22}$$

$$G_2 = g_2 \frac{a_2}{a_1} \tag{2.23}$$

ensures that the two systems will have the same diffraction loss, same resonant frequency and scaled intensity mode patterns. The stability criterion can also be written in terms of G_1 & G_2 or g_1 & g_2:

$$0 < G_1 G_2 < 1 \quad or \quad 0 < g_1 g_2 < 1 \tag{2.24}$$

The fields of the modes in stable resonators are more concentrated near the resonator axes than those in unstable ones and so, the diffraction losses of stable resonators are much lower. The smoothness of the stable to unstable resonator regime transition decreases with increasing Fresnel number. For a given Fresnel number, a confocal resonator system has the lowest diffraction loss, but it is important to remember that even minor deviations from this case may lead to unstable resonators, as is evident from Fig. 2.1.

Since the transverse field distribution of any general resonator mode cannot be solved analytically by finding the eigenfunctions of the integral equations, numerical solutions are possible, either by the method of successive approximations or the method of kernel expansion. The method of successive approximations is useful for lower-order modes wherein the resonator is initially excited by a wave of arbitrary distribution which undergoes multiple reflections and loses energy by diffraction leading to a quasi-steady state field distribution, which has the lowest diffraction loss for the specific resonator geometry. The method of kernel expansion yields solutions of both lower order and higher order modes.

The diffraction loss (α)

$$\alpha = 1 - |\gamma|^2 \tag{2.25}$$

and the phase shift (β)

$$\beta = angle \; of \; \gamma \tag{2.26}$$

help us in determining the quality factor Q and the resonant frequency by

$$Q = \frac{2\pi d}{\lambda \alpha_t} \qquad (2.27)$$

and

$$\nu/\nu_0 = (q+1) + \beta/\pi \qquad (2.28)$$

if the total resonator loss is small. It has been seen that the loss of the lowest order mode of an unstable resonator is independent of the mirror size and shape to first order.

2.2 Diode lasers

Most atomic physics research involves looking at the interaction of light and atoms, for which laser sources that can be tuned to specific atomic transitions are essential. Earlier, such laser sources were tunable dye lasers, which have now been replaced by semiconductor diode lasers due to the improvements in their reliability, power, wavelength coverage, and cost efficiency. Diode lasers also have better amplitude stabilities which make them suitable for sensitive absorption and fluorescence measurements.

2.2.1 Basic Laser Characteristics

Diode lasers are very small devices capable of output powers with high electrical to optical efficiency. The laser beam is generated by sending an injection current through the active region of the laser diode between the n & p-type cladding layers, producing electrons and holes which recombine and emit photons.

The emission wavelength of the laser depends on the band gap of the semiconductor material, and it is broad w.r.t. atomic transitions.

The spatial mode of a laser is defined by a narrow channel in the active region that confines the light. The confinement of the transverse laser mode is achieved either by the spatial variation of injection current density (gain-guided lasers) or by the spatial variation in the refractive index (index-guided lasers).
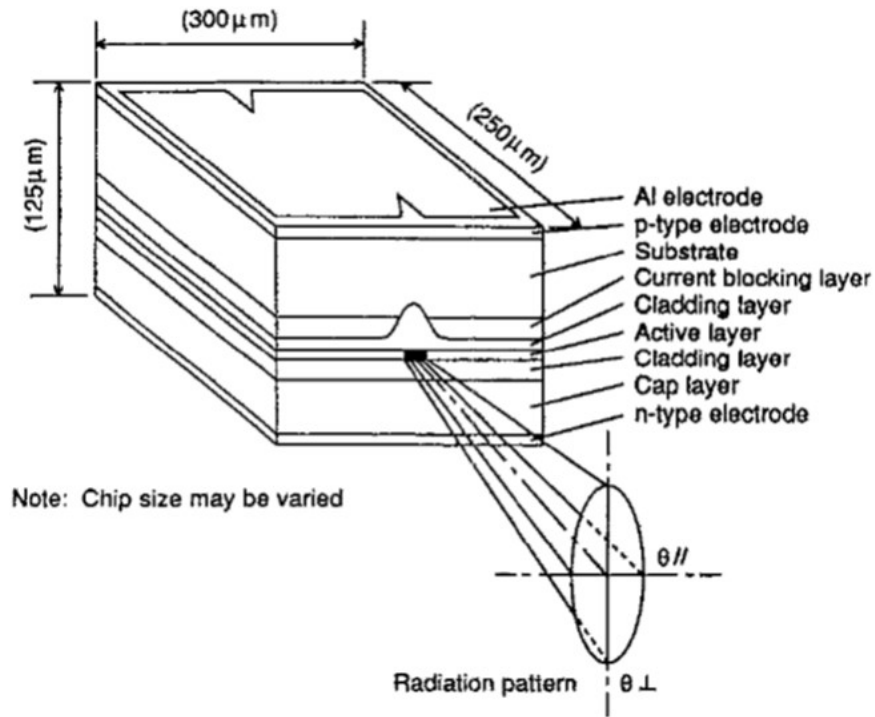
Figure 2.4: Typical diode laser - different semiconductor layers and dimensions [11].

2.2.1.1 Beam spatial characteristics

Due to the emanation of the light from a small rectangular region ($\sim 0.1\mu$m), the output laser beam has a large divergence and an oval radiation pattern (see Fig. 2.4 & Fig. 2.6).

At the full width at half maximum of intensity, a typical output beam has a divergence angle of 30° and 10°, in the perpendicular and parallel directions respectively, the difference arising from the variation in the spatial extent of the junction in the two directions w.r.t. the beam size. The output beam of most diode lasers also suffers from astigmatism. The first collimating lens used for typical diode lasers does not lead to Gaussian beam profiles. A Gaussian beam can be obtained by using corrective lenses and spatial filtering but at the cost of losing power.
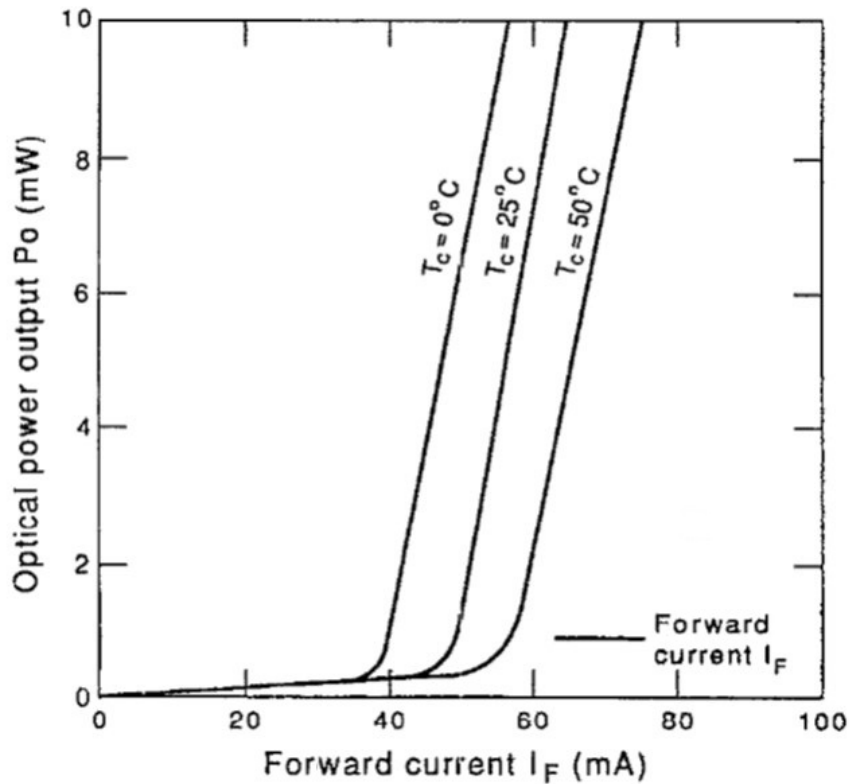
16

Figure 2.5: Laser beam output power vs injection current for a typical semiconductor diode laser [11]. [Note: Refer to Fig. 4.8 for my measurement of the lasing threshold]

2.2.1.2 Tuning characteristics

The wavelength of a diode laser is essentially determined by the bandgap of the semiconductor material, along with the junction temperature and the current density. Since the semiconductor bandgap is not accessible to the laser user, the broad range of the laser's wavelength cannot be controlled. Commercial lasers usually tune over a wavelength interval of about 20 nm, and therefore it is necessary to purchase lasers which are doped to operate in the required wavelength range. The optical path length of the cavity and the wavelength dependence of the gain curve vary with temperature. Consequently, the laser frequency also tunes with temperature similar to a step function with sloping steps, where the slope of each step represents the tuning of a cavity mode, while the jump between steps represents mode hopping due to the shifting of the gain curve.

These spectral gaps, of about 0.35 nm, are a serious drawback of using diode lasers and
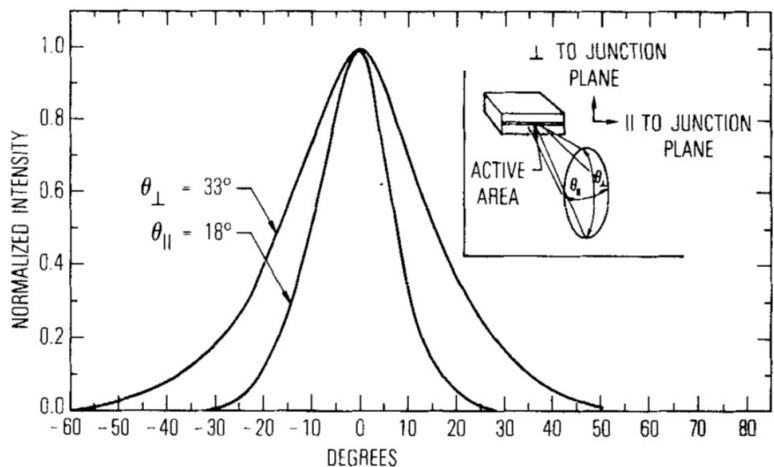
17

Figure 2.6: The output beam of the diode laser is highly divergent because of the small size of the active (lasing) area. Since the lateral dimension of the active area is usually larger than the transverse dimension, the angular spread of intensity in the lateral direction, $\theta_{\parallel}$, is less than the angular spread in the transverse direction, $\theta_{\perp}$. [16]

they are extremely sensitive to optical feedback, which can be used properly to reduce or eliminate the problem.

Typical room temperature lasers operate within a range of ± 30 K from the room temperature. Heating up the diode laser leads to higher lasing power which in turn leads to higher energy dissipation, increasing the chances of catastrophic failure of the laser diode. The laser wavelength also depends on the injection current. The injection current affects the diode temperature and also changes the refractive index by altering the carrier density, both of which in turn vary the wavelength. For timescales greater than 1 μs, the tuning of the injection current leads to a rapid change in the temperature by Joule heating of the junction, while the relatively low change in the carrier density makes the influence of the change in the refractive index on temperature insignificant.

An important advantage of diode lasers over other optical sources is that their amplitude and frequency can be modulated rapidly with ease by altering the injection current. However, the modulation of the injection current leads to coupled amplitude modulation and frequency modulation. Even though the sensitivities of AM & FM are different, the relative phase between AM & FM changes as a function of the modulation frequency. The FM & AM response is approximated to be linear with the injection current, and since the FM sensitivity
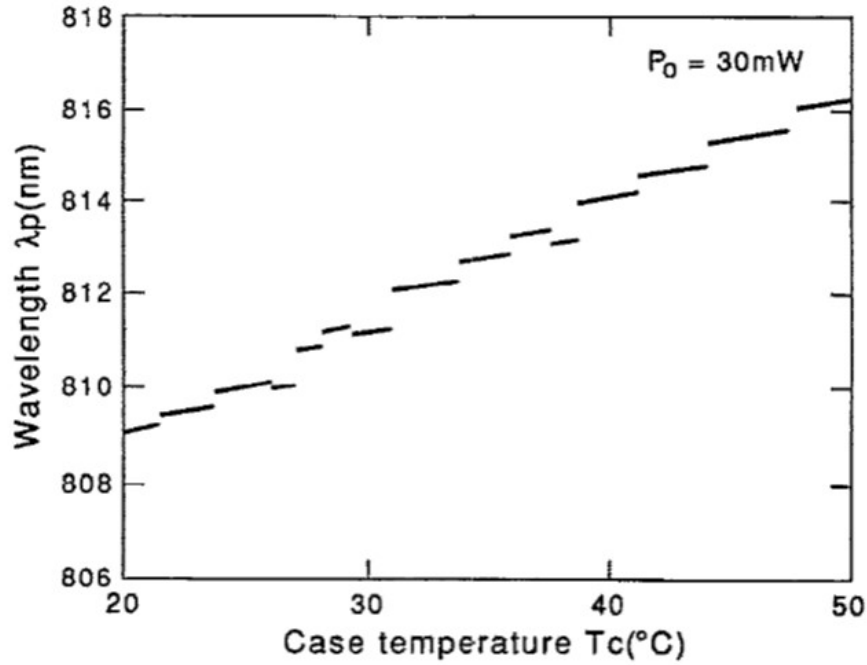
18

Figure 2.7: Laser output wavelength vs laser temperature [11].

is about an order of magnitude higher than the AM sensitivity, the amplitude change is ignored in most atomic physics experiments. This makes it possible to scan the laser over a large range of frequency for spectroscopic applications by appropriately altering the injection current.

2.2.1.3 Visible red lasers

Visible diode lasers operating near 670 nm, i.e. red light, are useful for diverse applications since they are near the resonance line of the Lithium atom at 671 nm, but they have a broad spectral width since they are usually gain-guided rather than index-guided. Typically they run over multiple modes, and even in the limited regions of single-mode operation, the linewidth of unstabilized devices is greater than or equal to 300 MHz. The large asymmetric divergence in their transverse mode structure produces, without any compensatory optics, elliptical beam shapes.

2.2.2 Using Diode Lasers in the Laboratory

2.2.2.1 Mounting a diode laser

The two most crucial initial considerations for mounting a diode laser, regardless of application, are temperature control and optical feedback. It is important to minimise unwanted optical feedback as best as possible, and also provide controlled optical feedback for frequency control, if desired. Along with this, the mounting design needs to keep the temperature of the laser as stable as possible. A reasonably simple, compact and mechanically rigid diode laser mount, as shown in Fig. 2.8, contains a thermoelectric heater/cooler, a sensing thermistor and a collimating lens, usually an aspheric lens, in a threaded longitudinal track for focussing adjustment.
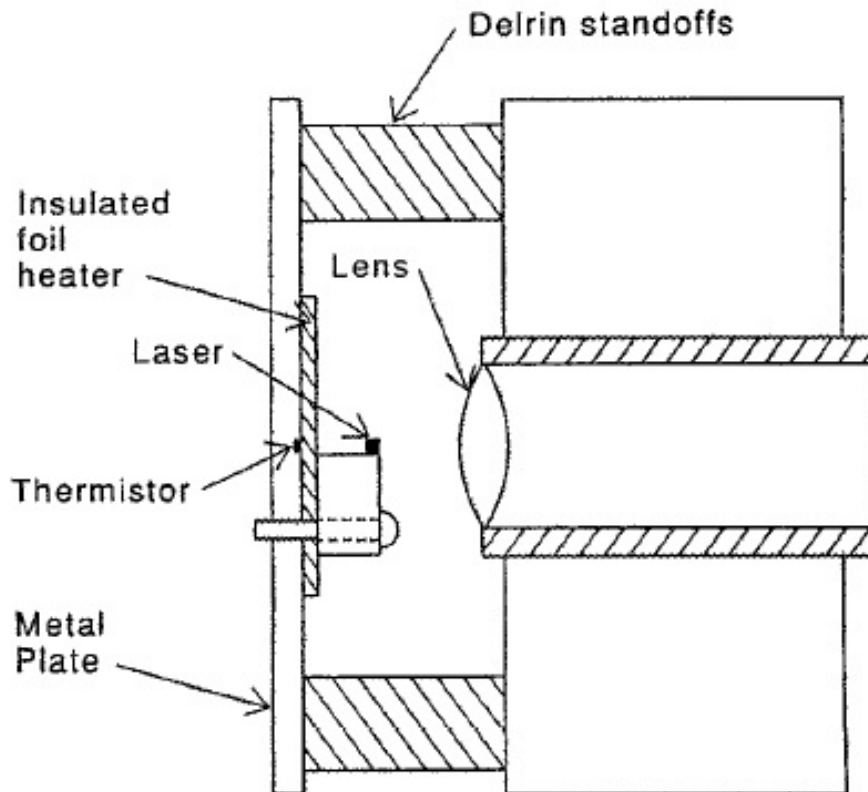

Figure 2.8: A simple diode laser mount [11]

2.2.2.2   Temperature and current control

The reproducibility of the laser system's performance depends on the temperature stability since the laser output frequency is directly dependant on the temperature. If external optical feedback is provided to the laser diode, or in the case of backscattering to the laser from the collimating lens, the laser frequency is sensitive to the position of the optical elements. Poor temperature control can cause unwelcome changes in the optical path length and phase of the feedback light, thereby affecting the laser frequency. Therefore, it is essential to have a robust temperature control system, preferably at the base of the laser mount itself. For this purpose, simple temperature control servo loops can be designed which basically use a thermistor as one leg of a balanced bridge circuit, and amplify any voltage across the bridge to drive a heater or cooler. If the sensing thermistor and the laser diode are in close proximity to the heater and the thermal disturbance from thermal radiation or air currents is minimised, such a simple circuit can achieve temperature stabilities on the order of 1 mK.

The final essential element in setting up a diode laser is the current control circuit. Though circuit designs vary with the specific requirements of different experiments, in every case, there needs to be a low-noise current source and adequate protection against undesirable transients that can destroy the laser. It is important to mount this protection diode as close to the laser diode as possible, as even a fraction of a metre of unshielded cable between the two can lead to the destruction of the laser by a high voltage spark.

2.2.2.3   Tuning to an atomic transition

While using diode lasers in most atomic physics experiments, the primary difficulty lies in tuning them to the desired wavelength, usually corresponding to some atomic transition. To do so, the laser current is set to the desired operating value, and then the temperature of the laser is tuned to the correct value by observing the wavelength of the laser on a spectrometer. When the laser is in proximity to the correct temperature, the current is rapidly ramped back and forth over a large range, while simultaneously adjusting the mount temperature in small increments to arrive at a combination of current and temperature that produces the desired wavelength. The fluorescence from an atomic absorption cell is used to determine when the required transition wavelength is reached. There may not be any current and temperature combination that leads the laser to a specific wavelength, depending on the

presence or absence of tuning gaps. On the other hand, when multiple possible combinations exist, maximum power can be attained when the laser current is high, whereas, for low power requirements, it is advisable to pick a low current point to maximise the lifetime of the diode laser.

2.2.2.4   Avoiding unwanted optical feedback

Diode lasers are extremely sensitive to optical feedback in contrast to other types of lasers, and this is both a blessing and a curse. This high sensitivity to optical feedback arises from a combination of factors - a very flat gain curve as a function of wavelength, low cavity finesse, and a very short cavity. Consequently, the overall gain of the laser system has an extremely weak dependence on wavelength, and with few photons in the cavity, the lasing frequency is easily perturbed. Additionally, the laser acts as a photodetector when light returns to it, which generates more carriers at the junction and affects the net laser gain. Lasers which have a reduced reflectance coating on the output facet are more sensitive to optical feedback than uncoated lasers. However, if a laser is set up to stabilise the wavelength through optical feedback, it is less sensitive to stray feedback light. If a simple re-positioning of optical elements does not avoid unwanted feedback back to the laser, an optical isolator needs to be used. To ensure beam power is not wasted, it is necessary to use a Faraday isolator if the incident and return light have different polarisation. A Faraday isolator allows light to pass in only one direction and breaks time-reversal symmetry.

2.2.2.5   Ageing behavior

Laser death is caused by either ageing, a gradual change in the laser behaviour over time, or catastrophic failure, which means user-induced destruction of the laser, usually not deliberate. Operation of diode lasers at high temperature and high current accelerates ageing. A very slow change in laser behaviour due to ageing is the gradual movement of the tuning steps, which may be as large as 30 MHz/h, most likely due to the increase in thermal conductivity between the laser and the heat sink and changes due to non-radiative recombination in the laser. In such cases, the current and/or the temperature needs to be readjusted occasionally to keep the laser on the atomic resonance. It may eventually happen that the gradual shift leads to losing the transition entirely, or interestingly, such a shift can also lead

to a previously untunable laser become amenable to tuning with age. Faster changes evident with ageing are the tendency of the laser to emit in more than one longitudinal mode, and the gradual increase of the spectral width of single mode output from an initial 20-30 MHz up to several hundred MHz.

2.2.2.6   Catastrophic failure modes

Catastrophic failure can be brought about on a diode laser by even a brief transient that causes too much current flow or too large a back voltage across the junction. Care must be taken to avoid switching transients arising from accidental disconnections, even after a protective circuitry has been put in place. To avoid laser death from transients originating from discharges of static electricity or high voltage arcs nearby, good grounding and shielding procedures must be put in place. It is also important to not touch the laser itself or its tiny current leads. Due to the low capacitance of the diode laser, even a little bit of reverse voltage across the diode's junction can lead to catastrophic failure.

2.2.3   Controlling and Narrowing Laser Output Spectra

A host of optical and electronic techniques have been developed to narrow the linewidth and control the central frequency of diode lasers. The essence of optical feedback methods is the idea that increasing the quality factor of the laser resonator will reduce the linewidth, and the simplest implementation of such a spectral narrowing scheme is to reflect back to the laser a small part of its output power. The basic electronic method, on the other hand, controls the laser's frequency by providing feedback to the injection current of the laser. Both these methods have severe limitations in their applicability, and more successful methods are utilised commonly, which are mentioned below.

2.2.3.1   Extended cavity diode lasers

It is possible to narrow a laser's linewidth and control its oscillation frequency by providing external frequency-selective optical feedback. Such systems, also known as pseudo-external cavity lasers, don't need the external feedback for the laser to oscillate but the systems

operate such that the external feedback dominates over that from the low-reflectance facet. Only one of the output facets of a diode laser may be anti-reflection coated, but the coating is not mandatory for such a setup. A bad coating may lead to the death of the diode laser due to its inability to withstand high power densities, which would be used if there was such a coating.
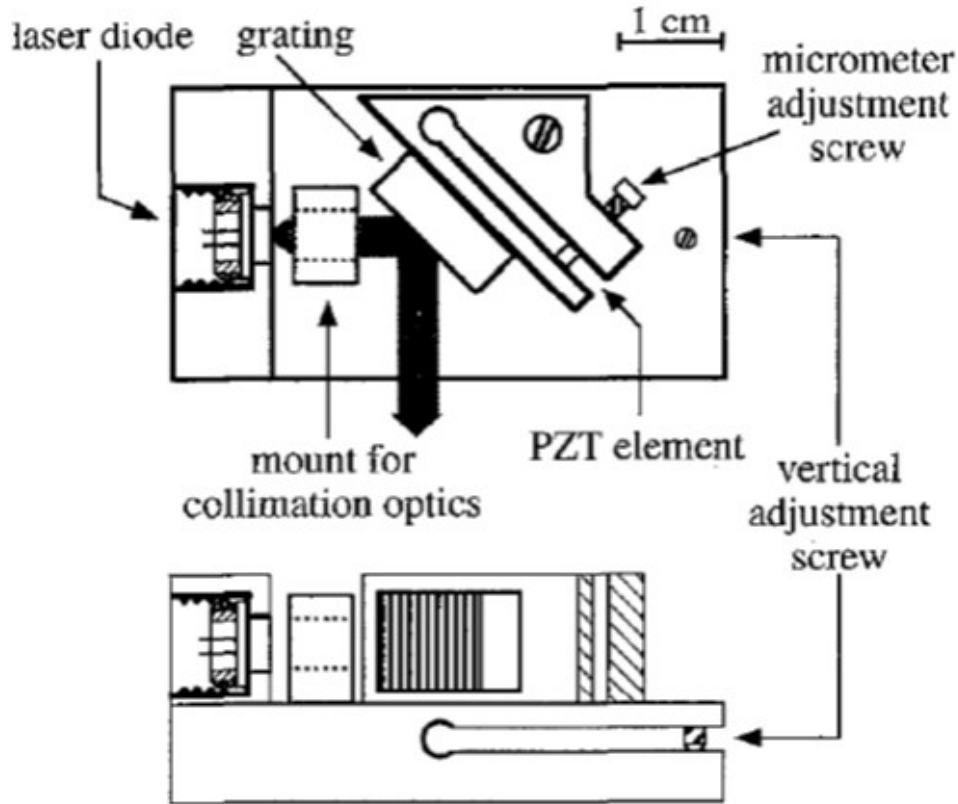

Figure 2.9: Schematic of the Haensch design of a grating-stabilized extended cavity diode laser [32]

Their fundamental linewidths are typically less than or equal to 100 kHz, and the grating allows tuning over a range larger than what is possible by temperature tuning. The tuning can also be continuous over a much larger spectral range ($\sim$80 GHz), and it is relatively easy to set and maintain the laser frequency at particular atomic transitions. It is possible to obtain continuous tuning by mounting the grating in a manner such that upon its rotation, the change in the cavity resonant frequency due to the change of the cavity length matches the angle tuning of the grating [20]. By reducing the percentage of feedback power to increase the output coupling, the range of continuous tuning and the maximum range the laser wavelength can be pulled from its gain peak reduces.

2.2.4 Applications

2.2.4.1 Trapping and cooling atoms using diode lasers

Cavity and grating-stabilised diode lasers have also been pivotal in cooling and trapping neutral atoms, which require several different laser frequencies with linewidths of less than 1 MHz [25].
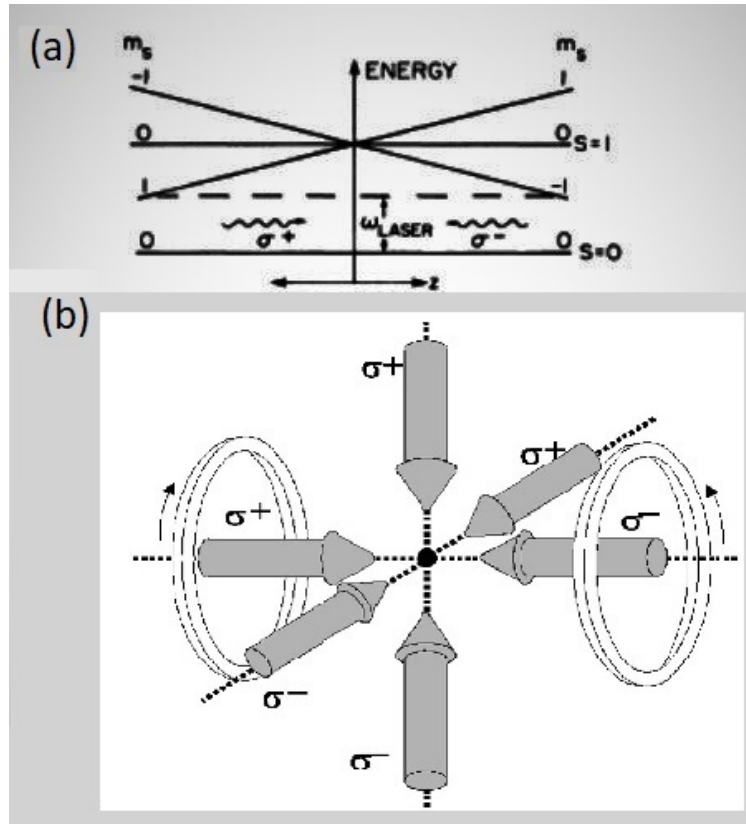

Figure 2.10: Principle of a Magneto-Optical Trap - (a) Energy-level diagram of a hypothetical atom having spin $S = 0$ ground state and spin $S = 1$ excited state, immersed in a magnetic field $B_z(z) = bz$. The frequency and polarisation of the counterpropagating laser are chosen to produce damping and restoring forces for the atom's z-axis motion. (b) Trapping scheme in 3D: A spherical quadrupole field is generated by two coils of opposing current placed along the z axis. The field along the axes, indicated by the light arrows, is parallel to its respective axis. Laser light, indicated by the heavy arrows, counterpropagates along x, y and z directions, and is polarised as shown with respect to the axis of propagation. [29] [35] [36]

Atomic samples of caesium containing 5 x 10^7 atoms were cooled to a temperature of 100 μK using the optical molasses technique [26]. In this technique, a three-dimensional standing wave tuned to the red side of the caesium resonance line creates a viscous optical medium for the atoms, confining the atoms before they can diffuse out of it [25].
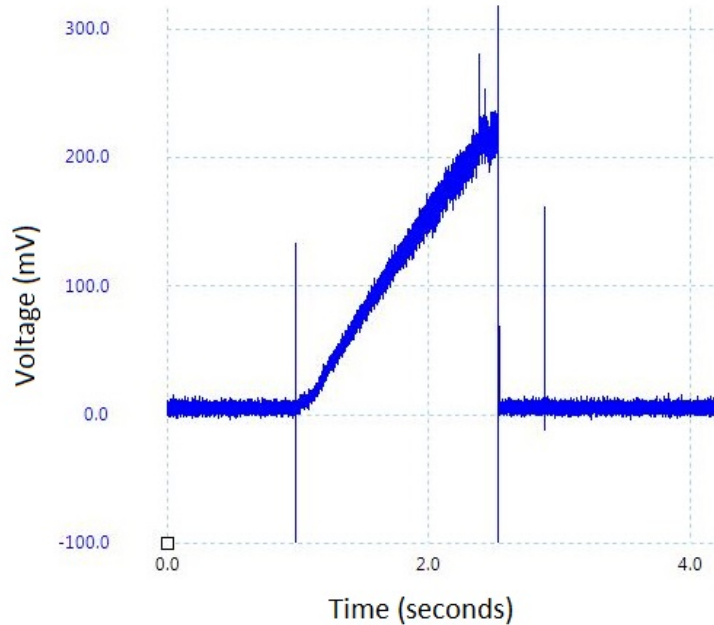

Figure 2.11: Fluoroscence signal of Lithium atoms being captured in a Magneto-Optical Trap

This method is based on the original idea of cooling atomic samples by using counter-propagating laser beams [27].

In the case of lithium, 4 x 10^8 fermionic ^{6}Li atoms have been confined simultaneously with 9 x 10^9 bosonic ^{7}Li atoms in a magneto-optical trap based on an all-semiconductor laser system by sympathetic evaporative cooling and Sisyphus cooling to 1 mK. [28]

In both optical molasses and atom trapping experiments, the ease of rapid frequency changes and the very low amplitude noise of diode lasers has proved invaluable.

2.2.5 Summary

Inexpensive, simple and highly reliable diode lasers have proved to be valuable tools for atomic spectroscopy, offering continuously tunable sources of radiation with linewidths less than 100 kHz and output powers of 100 mW or more, and covering much of the near infrared region to the visible part of the electromagnetic spectrum.

2.3 Lithium atom

Lithium has two stable isotopes ^{7}Li, a boson and ^{6}Li, a fermion. The natural abundances are 92.5% for ^{7}Li and 7.5% for ^{6}Li. Lithium is the third element in the periodic table, and the lightest of the alkali metals. Alkalis have a single electron in their outermost electronic shell (an s-shell), and so they have a simple atomic structure. ^{6}Li has a nuclear spin of I = 1, ^{7}Li of I = 3/2. The energy levels at zero magnetic field of ^{6}Li and ^{7}Li are represented in the figure below, and the optical transition from the 2s orbital to the 2p is at 671 nm. It is important to have an optical transition frequency that is easy to produce for laser cooling. The optical transition frequency of the Lithium line at 671 nm enables the use of reliable diode laser sources for generating light at this wavelength. [31] The fine structure splitting between the $2^2P_{1/2}$ and the $2^2P_{3/2}$ state is about 10 GHz. Incidentally, the isotope shift of the 2S $\rightarrow$ 2P transition is also of 10 GHz, and the D1 line ($2^2S_{1/2} \rightarrow 2^2P_{1/2}$) of ^{7}Li is almost tuned with the D_2 line ($2^2S_{1/2} \rightarrow 2^2P_{3/2}$) of ^{6}Li. The natural linewidth of the optical transitions is $\Gamma = 2\pi \times 5.9$ MHz for both isotopes, from which we can conclude that the hyperfine levels of the $2^2P_{3/2}$ are not resolved since their splitting is smaller than the linewidth Γ [12].

Lithium is used in the experiments due to three advantages[14]:

- It has two stable isotopes which can be cooled down to very low temperatures.

- It has several broad Feshbach resonance, which gives good control over interaction strength.

- It has a long life time in the superfluid phase, e.g. ^{6}Li has a lifetime of about 10 seconds in the superfluid phase.

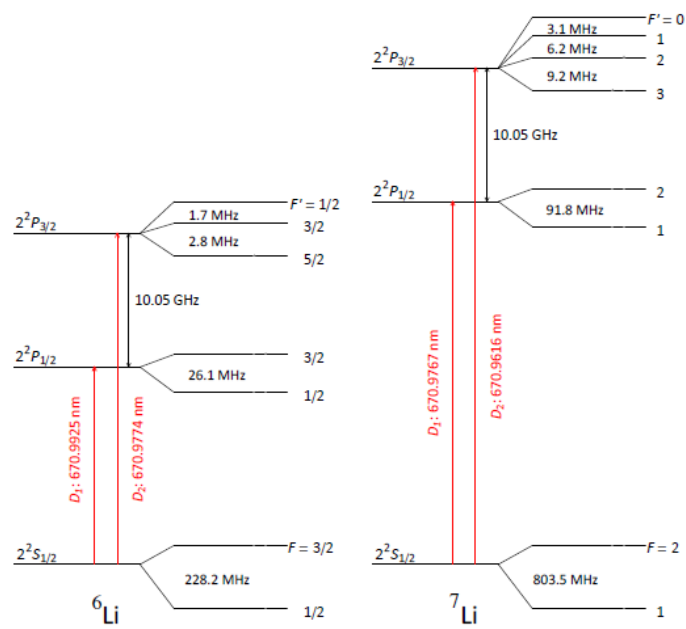Figure 2.12: Atomic transitions in Lithium [13]

Chapter 3

Design of the laser system

3.1 Setup

The design of the optical system has been carried out with the objective of having a continuous wave laser source that has a high output power while also maintaining a narrow linewidth for the output wavelength. In order to achieve these conditions with conventional semiconductor diode laser sources, we have used a master oscillator power amplifier (MOPA) scheme, where an amplifying laser with a high-output beam power is phase-locked to the output laser beam from a low-power narrow-linewidth single-frequency master laser [37]. By unidirectionally injecting the output beam of the master laser to the optically amplifying slave laser, it is possible to obtain a final laser output beam with high beam power as well as

29

a narrow-linewidth wavelength spread. A critical requirement of the injection-locking mechanism is to ensure that a negligible amount of the amplifying laser's beam power is sent back to the master oscillator laser, so that the frequency stability of the master laser is preserved, and self-oscillation of the amplifying laser is prevented, a condition known as non-reciprocal coupling. In principle, this type of coupling implies that the oscillation frequency can be tuned on the master laser and the output power level of the laser system can be assigned through the slave laser.

Even though the architecture is more complex than a single laser directly producing the required laser output power, there are significant advantages of employing the design, as listed below:

1. By decoupling the required laser performance characteristics from the generation of high power, it is easier to attain the necessary linewidth and wavelength tuning range than it would have been if additional optical components required for achieving these characteristics had to withstand high optical intensities as well.

2. It can be used to obtain a high power laser output using available laser sources instead of having to purchase or develop customized sources for every application.

3. It is possible to minimize spectral and spatial mode instabilities in the final output laser beam as they scale up with the drive current of the primary oscillator laser.

The setup required for the optical system has three major components - a master laser, an optical isolator, and a slave laser, along with associated electronic and optical elements. A schematic of the optical setup is shown below:

3.1.1   Master Laser

The master laser is a semiconductor diode laser of the type AC-06283, assembled in an extended cavity laser configuration, and mounted in a metallic casing in the lab to isolate it from air current fluctuations and other disturbances. The spectrum of the master laser is centered at 660 nm[12]. It can achieve laser output power in normal conditions of up to 120 mW in the continuous mode. To obtain light on the transitions of lithium at 671 nm, the diode is heated up to approximately 70°C without reducing the diode's performance
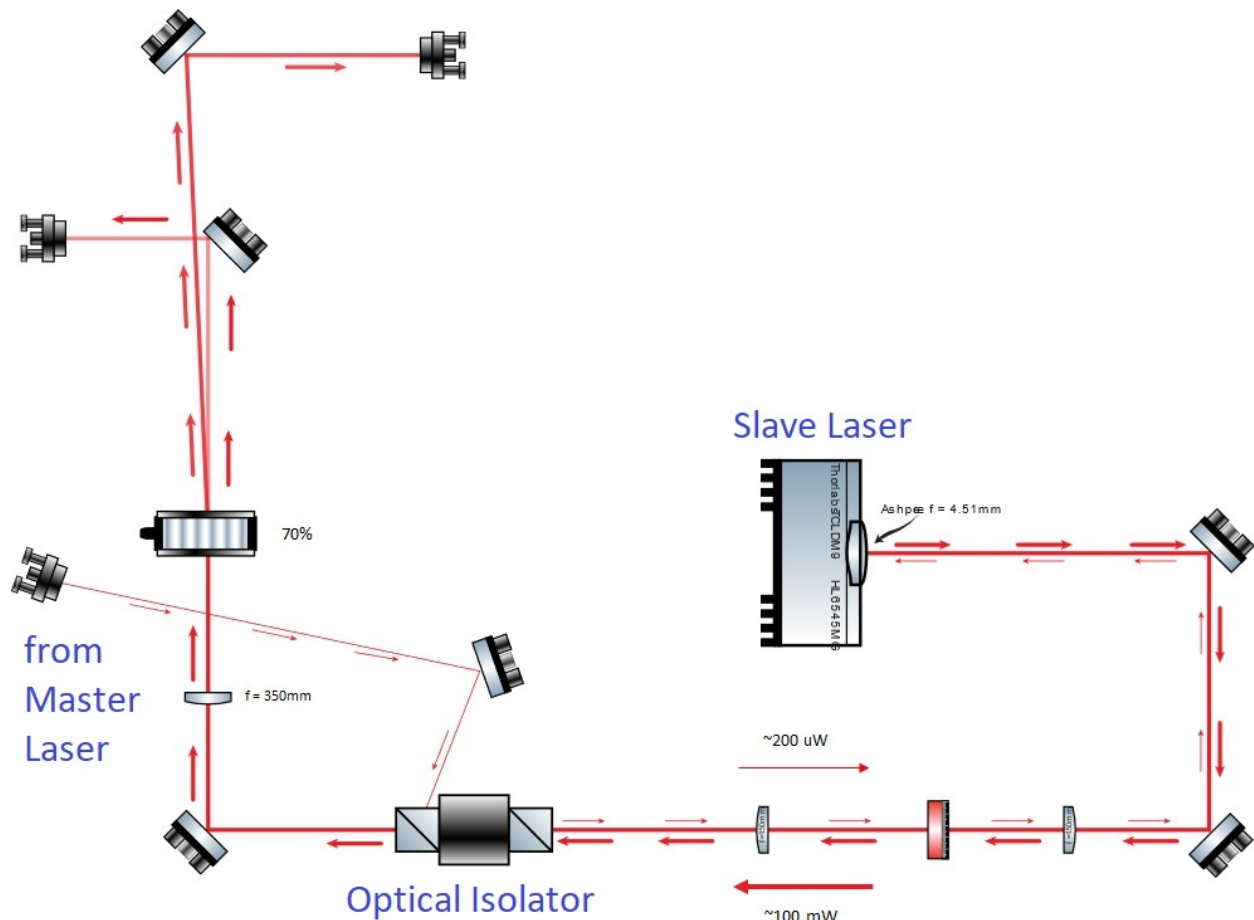
Figure 3.1: Schematic of optical system [15]

significantly. By doing so, there is a broadening of the electronic bands which brings the valence and the conduction band closer to each other, leading to a shift in the emission line of the laser to higher wavelengths. The key elements include an aspheric collimating lens in front of the laser's output facet, a diffraction grating, a Peltier heating / cooling element, a thermistor, and associated protection and control circuitry.

3.1.2 Optical Isolator

An optical isolator is an optical component which allows the transmission of light in a single direction, akin to a diode in electrical circuits. The primary unit is the Faraday rotator inside, which provides non-reciprocal polarization rotation while also maintaining
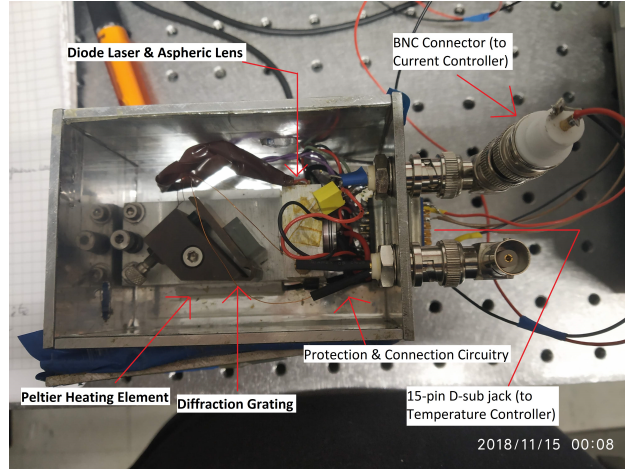
Figure 3.2: Master diode laser

linear polarization of light. The incident beam is aligned with the magnetic field direction when entering the optical isolator so that it has a 45° rotation, while the beam reflected back from the slave laser is aligned in the opposite direction and hence suffers a rotation by -45°, cumulatively ensuring that the final beam is perpendicular to the initial polarization of the incident light beam. Therefore, this component ensures that unwanted optical feedback does not enter and damage the master laser, maintaining the fidelity and the efficiency of the MOPA design configuration, with a typical attenuation of the return light by 40 dB in case of a single isolator and 65 dB in case of a double isolator.

3.1.3 Slave Laser

The slave laser is used as an optical power-amplifier in the Master Oscillator Power Amplifier (MOPA) scheme since the master laser has a narrow wavelength linewidth but with a lower power. The slave laser, on the other hand, has a higher power but at the cost of a broader linewidth. To have both higher power and narrow linewidth, the slave laser is injection-locked to the master laser which ensures that it lases in the narrow linewidth corresponding to the master laser.

32

3.1.4 Temperature Controller

One of the major considerations for setting up a diode laser is temperature control, as discussed earlier in 2.2.2.1. We use the Thorlabs TED200C Thermoelectric Temperature Controller to control the temperature of the master laser diode. The TED200C temperature controller can drive the thermoelectric cooler in the Master laser setup, based on the Peltier effect, with a current control range upto $\pm$ 2 A with a resolution of 1 mA, and a maximum output power of 12W [33]. In our case, it is used with a Thorlabs TH 10K thermistor sensing thermistor, which has an operating temperature range from -50 °C to 150 °C [34]. The temperature controller's thermistance tuning range is from 10 Ω to 20 kΩ, with a resolution of 1 Ω. There is also an overheating protection circuitry wherein a heat sink inside the temperature controller is monitored and shut down if it exceeds a threshold limit.

The temperature controller has a PID servo loop where the different gain parameters of the feedback loop can be adjusted to optimize the stability and settling behaviour of the laser diode's temperature, as detected by the sensing thermistor in the master diode laser box. The proportional (P) gain is used to optimize the response of the feedback loop to reach the setpoint. The proportional gain measures an offset between the reference voltage and the output of the Wheatsone bridge voltage and amplifies it. It is re-inected in the loop with a negative sign to compensate for the error signal. The integral (I) gain integrates over the previous error, i.e. the voltage, to minimize the residual offset and provide a steady state offset regulation with higher precision. The derivative (D) gain modifies the dynamic response of the feedback loop in anticipation of the feedback response to achieve the setpoint. The ability to properly tune the PID parameters manually is crucial to achieving fast and long-term temperature stability. The essential theory behind a PID servo loop is discussed below.

3.1.4.1 PID Feedback Circuit

The proportional-integral-derivative (PID) control loop circuit is used as a feedback controller in servo circuits which require continuous automated modulation. A servo circuit is designed to maintain a system at a predetermined value, known as the setpoint, for extended periods of time. The PID circuit achieves this active control of the system by the generation of an error signal that is essentially the difference between the present value of a variable and

the value of the set point. The three parameters - P, I and D - are time-dependent error signals, where the proportional is related to the present error of the variable, the integral is the cumulative error of the variable integrated over time, and the derivative is a measure of the future change in the error behaviour [39].

$$P = K_p e(t) \tag{3.1}$$

$$I = K_i \int_0^t e(\tau)d\tau \tag{3.2}$$

$$D = K_d \frac{d}{dt}e(t) \tag{3.3}$$

The proportional gain is a direct response to the error signal, and hence, a larger proportional gain will induce a larger change in the error response. Too little proportional gain will be insufficient to change the system response to reach the set point. However, extremely large proportional gains will also reduce stability and increase oscillations of the output variable near the set point.

The integral control adds on to the proportional gain, as it is proportional to the duration of the error, in addition to the magnitude of the error signal. It is effective in eliminating the residual steady-state error remaining after only proportional control. However, large values of the integral control may lead to oscillatory instabilities.

The derivative control is used to predict how quickly the circuit response will change over time by calculating the derivative of the error signal, and by doing this, it attempts to reduce the overshoot and damp out oscillations due to the other two controls. With its slow response, high values of the derivative control can significantly reduce the system's ability to respond appropriately in time and increase the susceptibility to noise and high frequency oscillations.

$$u(t) = K_p e(t) + K_i \int_0^t e(\tau)d\tau + K_d \frac{d}{dt}e(t) \tag{3.4}$$

Each of these control parameters is computed and a weighted sum, depending on the P, I and D gain fractions, is then fed into the control device which consequently feeds this value back to the input signal to adjust the input variable in order to attain and maintain the system at the assigned setpoint. It is possible to choose a combination of these three parameters to control the circuit.
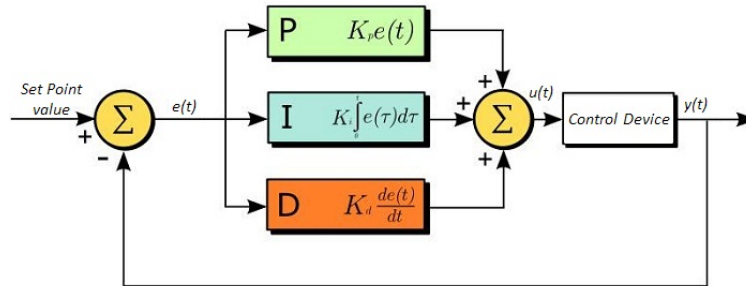

Figure 3.3: Block Diagram of a PID Servo Loop [39]

3.1.5   Current Controller

It is essential to have an appropriate current controller for setting up a diode laser, as discussed earlier in 2.2.2.1. For our purposes, we use the Thorlabs LDC200C Laser Diode Controller, with a current control and setting range from 0 to $\pm$ 200 mA and resolution of 10 μA. The current controller has essential laser diode protection, and can operate with all polarities of laser diodes in two modes - constant power and constant current. There is a precisely adjustable maximum current limit, and also an internal over-temperature protection wherein the output current is automatically disabled if the internal heat sink gets heated above a threshold, which can only be re-enabled after the internal heat sink temperature has reduced by 10 °C.

The current output is also automatically switched off if the connection between the laser diode and the current source is interrupted, and an internal electronic switch within the controller also short circuits the laser diode for additional protection. There is a soft increase in the laser current upon being switched on to avoid voltage transients, and a transient-free laser current is implemented by electrical filters, shielding the transformer, and carefully grounding the controller box.

Chapter 4

Experimental Realisation of Laser System

After learning the basics related to laser systems, I began working independently on the development of the optical system. The first step was to setup the master laser with appropriate current and temperature controllers and to begin lasing action, i.e. when stimulated emission dominates over spontaneous emission.

4.0.1 Controller & Master Laser Connections

To connect the Thorlabs TED200C Laser Diode Temperature Controller to the master laser, I had to solder the appropriate pins of the 15-pin D-sub jack on the master laser with those on the temperature controller. The connections involved shorting the status LED indicator pins, connecting the thermistor terminals to the master laser thermistor control, and connecting the temperature control elements in the controller to the Peltier element terminals in the master laser.

For the Thorlabs LDC202C Laser Diode Current Controller, I had to short the status indicator and ground pins together, and connect the cathode-grounded master laser diode BNC connector pins to the current controller.
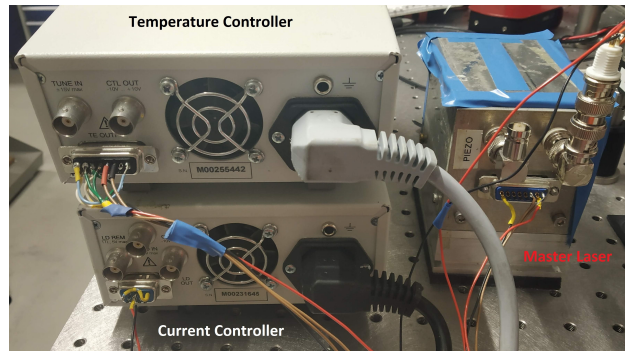

Figure 4.1: Connections for the Master Laser

4.0.2 Temperature Stabilization

After making the connections, I tried to achieve temperature stability on the temperature controller which supplies current to the master laser's thermistor and Peltier element in order to maintain the laser temperature at a given setpoint by tuning the proportional (P), integral (I) and derivative (D) controls on the feedback servo-loop, for which I used a tuning methodology analogous to a binary search algorithm. At first, all the P, I and D gains were set to zero. Subsequently the fractional P gain was changed to 0.5 and 1. By comparing the thermistance oscillation spread at the boundaries and the half-interval, the next tuning search was carried out by reducing the search interval to half of the previous one, in the appropriate direction. The same binary search method was used to find the optimum gain

settings of the I and the D parameter respectively. It is possible to execute the binary search algorithm, which has a worst-case logarithmic search time, since I have seen experimentally that the parameter gain vs fluctuation spread has a single global minima if the experimental conditions are fixed. I was able to achieve a thermistance stability on the order of $\pm 10 \ \Omega$ (0.2 °C) with P & D tuning, but after including all three, the stability is on the order of $\pm 500 \ \Omega$ ((10 °C)). The thermistance oscillatory behaviour during the tuning of the three controls is shown below, with the thermistance setpoint at 10.000 $k\Omega$ (25 °C).

Thermistance Oscillatory Range Variation with Proportional (P) Control Tuning in Temperature Controller PID Loop
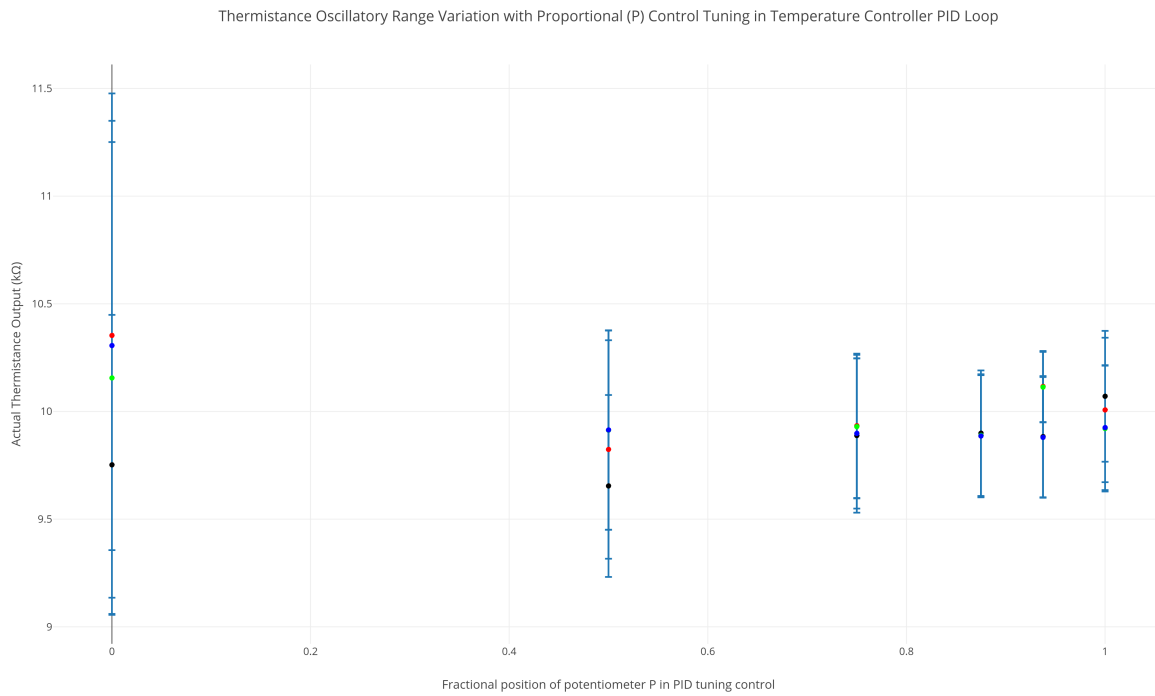
Figure 4.2: Thermistance vs P tuning

However, even after multiple attempts at reducing the thermistance variation to a more tolerable range, the oscillatory variation did not reduce below $\pm$ 100 Ω (2 °C). Oscilloscope measurements of the error signal showed a stable oscillatory behaviour within this range, which meant that the problem was not with the parameter tuning of the PID servo loop itself. To extract the cause of the problem, I then changed the temperature controller to a homemade ATMC temperature controller which also worked with a manually tunable PID servo loop. The ATMC temperature controller's temperature stabilization PID feedback loop runs essentially on a modified Wheatstone bridge.

The known leg of the bridge is discretely tunable, with coarse tuning done using 12

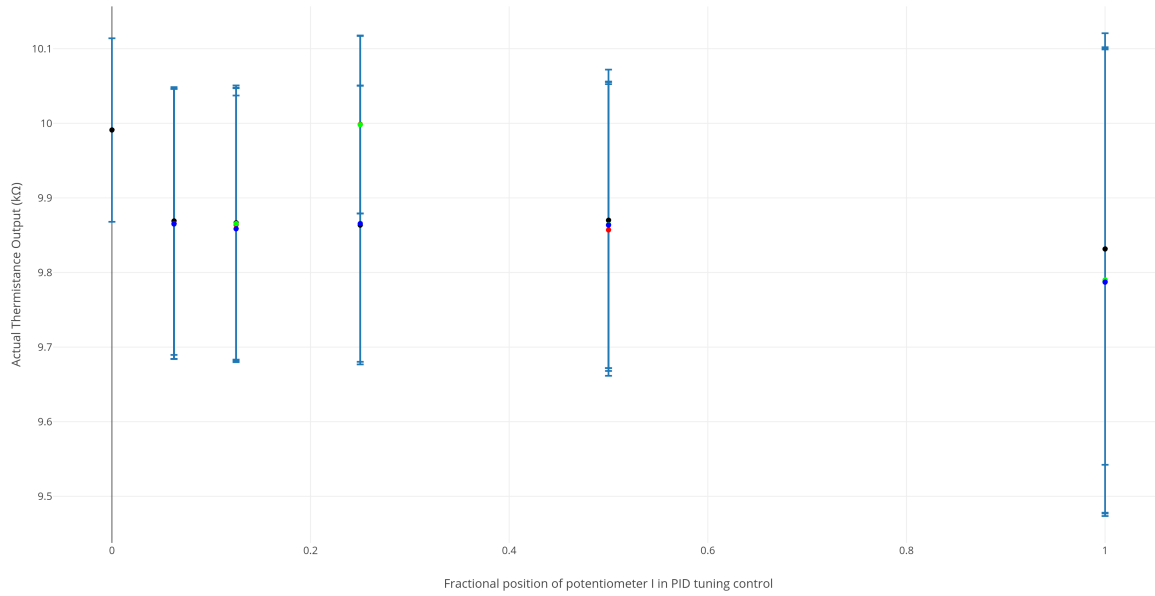Figure 4.3: Thermistance vs D tuning
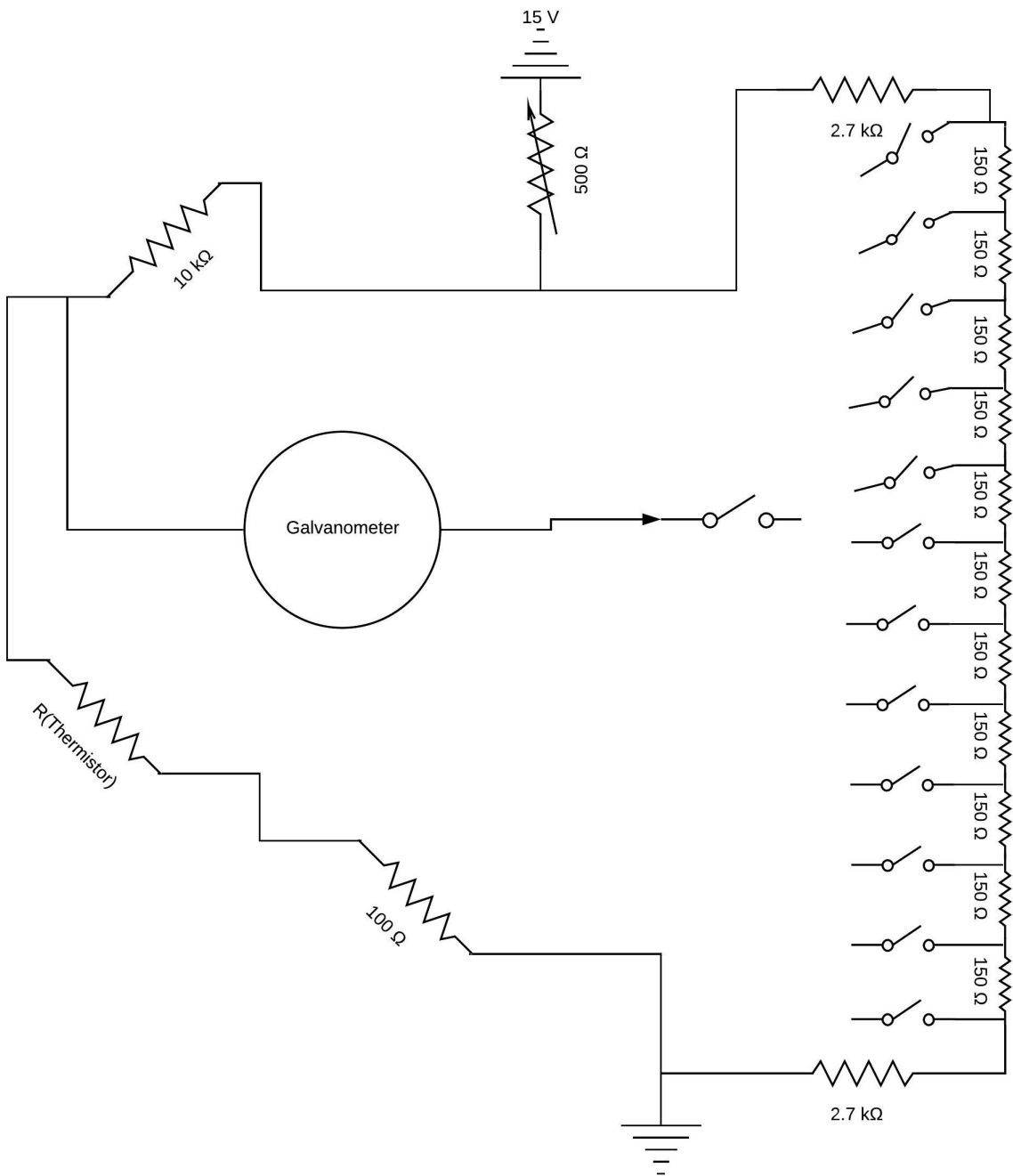

Figure 4.4: Thermistance vs I tuning

Figure 4.5: ATMC Temperature Controller - Simplified Circuit Diagram of Modified Wheatstone Bridge

resistors and the fine tuning done using a variable resistor, while the unknown leg is connected to the sensing thermistor of the master diode laser. An appropriate current is sent to the

Peltier heating element to heat / cool the diode laser, which in turns changes the thermistor's measured resistance, and the temperature stabilizes at a pre-fixed temperature setpoint - which is done using a fixed known resistor in one of the legs of the bridge - when the Wheatstone bridge is balanced. After making all the necessary connections with the master laser and the power supplies, and also tweaking the controller circuit to its original design, I measured the temperature stabilization behaviour with an oscilloscope and still found that the problem could not be resolved. By now, it seemed that the problem was not due to faulty wire connections or the temperature controller's PID loop parameter tuning. The Peltier heating element also performed appropriately, i.e. it heated up when a positive current was sent to it, and cooled down otherwise. In order to verify whether the sensing thermistor was working properly or not, I then affixed a 3-pin analog temperature probe to the wall of the diode laser's surrounding aluminium casing, and it showed that even though the sensing thermistor was following the correct real temperature profile of the diode laser, it was very imprecise, leading to a slow response to the temperature stabilization feedback loop, ultimately resulting in a large steady-state oscillatory spread of the thermistance.

Since the thermistor specifications mentioned a better precision, we decided to check if it was positioned correctly, so as to produce a temperature reading as close to the temperature of the diode laser as is possible. I found out that the sensing thermistor was thermally glued to the wall of the diode laser casing, and that it did not penetrate into the solid aluminium structure. This seemed to be the source of our problem, as this meant that the heat dissipation at the sensing thermistor due to air currents was not negligible, and also that there was a significant time delay between the actual temperature changes in the diode laser and its sensing by the thermistor. The position of the sensing thermistor should ideally have been inside the aluminium casing just at the base of the box, sandwiched between the Peltier element and the solid aluminium support, as conduction through aluminium was quick enough for the temperature just near the diode laser to be sensed by the thermistor, as well as being close to the Peltier element.

To achieve good isolated thermal contact of the thermistor with the metallic structure, I then set up another home-made master diode laser box, and placed the thermistor through a hole in the aluminium structure at the base of the box, just above the Peltier element. To connect the new master laser diode box, I had to create new connections from the different BNC and D-sub ports of the master laser box to those of the two controllers and an oscilloscope. I decided to develop a consistent wire connection scheme to enhance interoperability

and convenience at later stages, by ensuring that all new connections would have intermediate BNC ports so that any connection could be made by using already available BNC cables in the lab, which also reduced the requirement of procuring different adapters and connectors specific to each device. After redoing all the connections from the temperature and current controller, I tested this setup with the Thorlabs TED200C Laser Diode Temperature Controller, and the initial results showed a quick temperature stabilization from 3 kΩ (55 °C) to 15 kΩ (15 °C).

Subsequently, a more rigorous temperature stability test was conducted, and the temperature was stable for times of at least an hour. For the temperature stabilization test across the whole temperature tuning range of the Thorlabs temperature controller, I followed a simple protocol and video-recorded the procedure at 30 fps to have higher temporal resolution than is possible with the human eye. The thermistance setpoint in the controller was set to 12.500 kΩ, which is approximately equal to the room temperature of 20 °C, as given by the formula below.

$$R_t = R_{25°C}[e^{A+\frac{B}{T}+\frac{C}{T^2}+\frac{D}{T^3}}] \tag{4.1}$$

where, the constants A, B, C and D are available in [34].

The actual thermistance was then allowed to stabilise to the thermistance setpoint, within a variation of ± 1 Ω (0.02 °C). The connection from the controller to the thermoelectric heater was then broken, and the thermistance setpoint for the test temperature was set on the controller. As soon as the thermistance setpoint was fixed, the video recording was initiated, and the connection of the controller with the Peltier heater turned on. The whole stabilization process was recorded till the actual thermistance reached the thermistance setpoint, and did not fluctuate beyond ± 1 Ω for at least 30 seconds. The videos were then analysed, and the final thermistance stabilization point was chosen to be the first thermistance at which the fluctuations did not exceed ± 1 Ω for the minimum time duration of 30 seconds. Even though the whole process was continuously recorded, the plot below has points that were selected by equally dividing the full duration for each data set, with additional points (when required) near the setpoint to show the oscillatory or settling behaviour in more detail.

We can see here that at almost all thermistance setpoint values, the actual thermistance rises up and then stabilizes without overshooting at all. This can be attributed to optimum
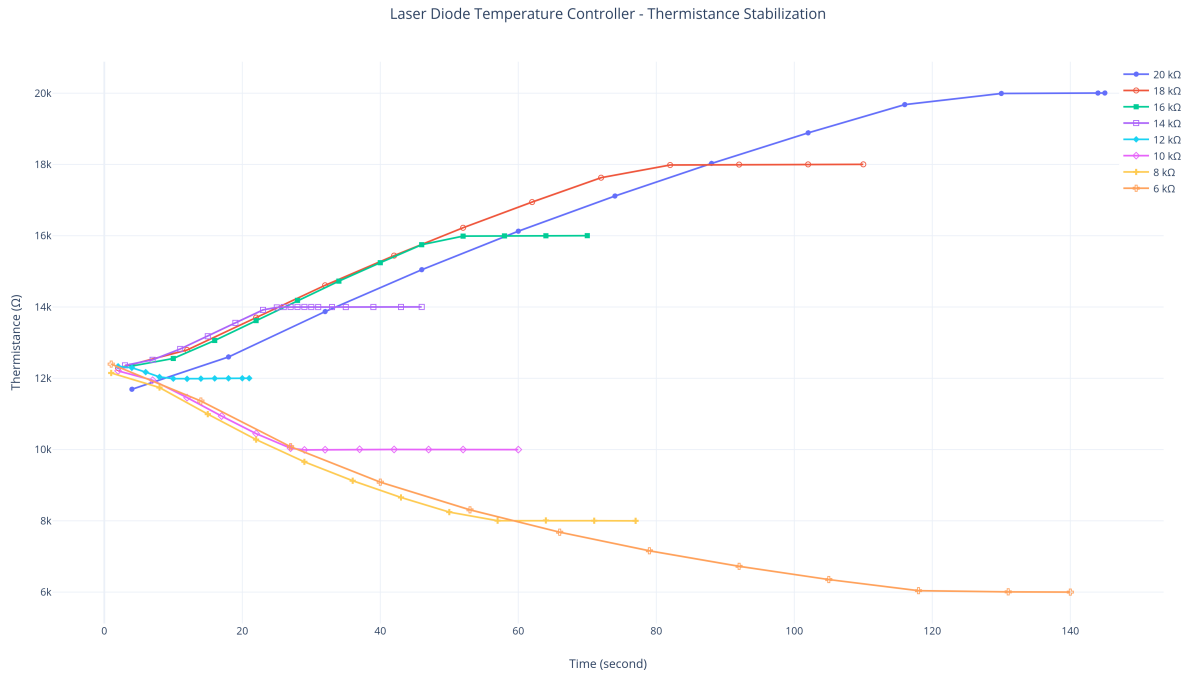
Figure 4.6: Laser Diode Temperature Controller - Thermistance Stabilization

tuning of the PID feedback control loop parameters, especially the derivative control which prevents overshooting. By carefully tuning the derivative control, I was able to achieve a situation analogous to critical damping in a simple harmonic oscillator where the oscillation damps in the minimum amount of time without any overshoot. It is evident and understandable that it takes more time to reach a setpoint that is farther away from the initial thermistance. It is interesting to note that it takes more time for the Peltier element to heat up and reach higher temperatures than to cool down by the same magnitude of the temperature difference, and it is especially marked at higher temperatures. The time required to stabilize to any temperature, except for the highest temperatures in our range, is fairly quick and the temporal stability at the set temperature is also quite good, in all cases being more than 1 hour. The master laser can therefore function efficiently within the range of 3 kΩ to 20 kΩ, which corresponds to the temperature range of 10 °C to 55 °C. The lowest thermistance that could be attained is 2.018 kΩ, which is about 65 °C.
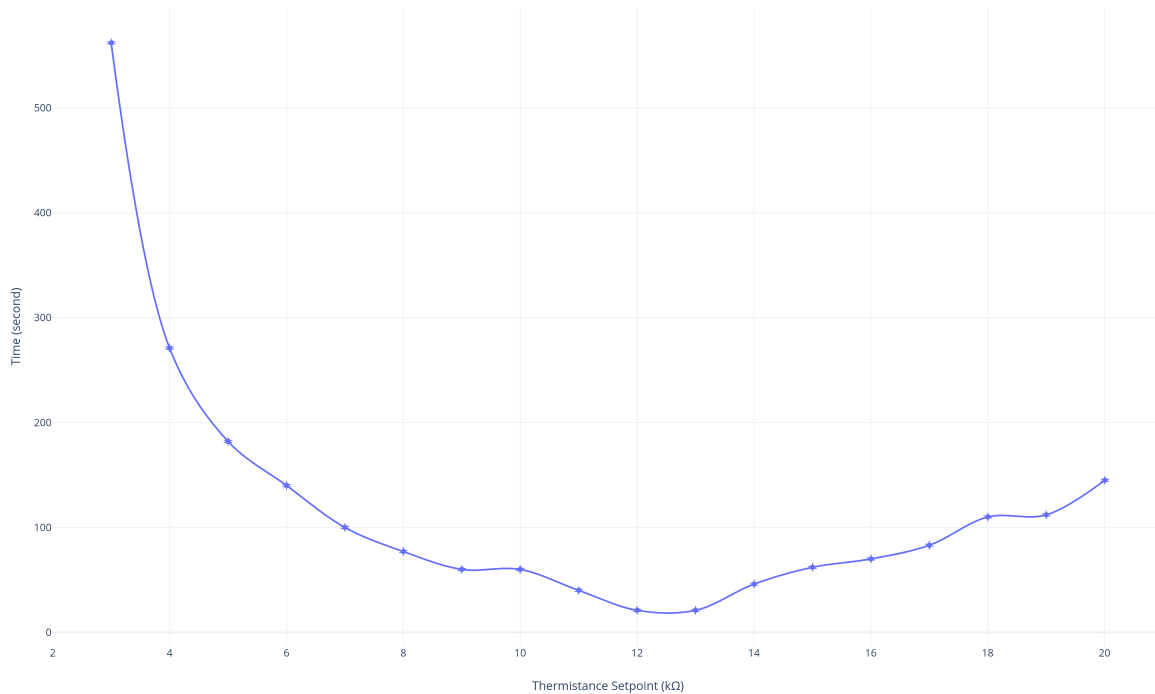
44

Figure 4.7: Laser Diode Thermistance Stabilization Time

4.0.3 Lasing & Beam Collimation

The lasing threshold of the master diode laser was also checked by observing the change in the laser output beam power with increasing injection current. The lasing threshold measurements were carried out for 3 different thermistances over the thermistance tuning range of the temperature controller. The plot below shows the result of the test, which is similar to the expected behaviour as shown in Fig. 2.5, with an additional plot line for the lasing power vs current behaviour at the unregulated room temperature, close to 11.404 kΩ.

From Fig. 4.8, we can see that the threshold injection current for the lasing action increases with increasing temperature, and that the power characteristics with current are similar at all temperatures (12 °C, 20 °C, 22 °C & 37 °C).

After the diffraction grating and the aspheric lens were adjusted to collimate the laser beam over a distance of about 3 metres, the laser's output beam's power was observed over a range of injection currents by varying the temperature and the distance between the detector
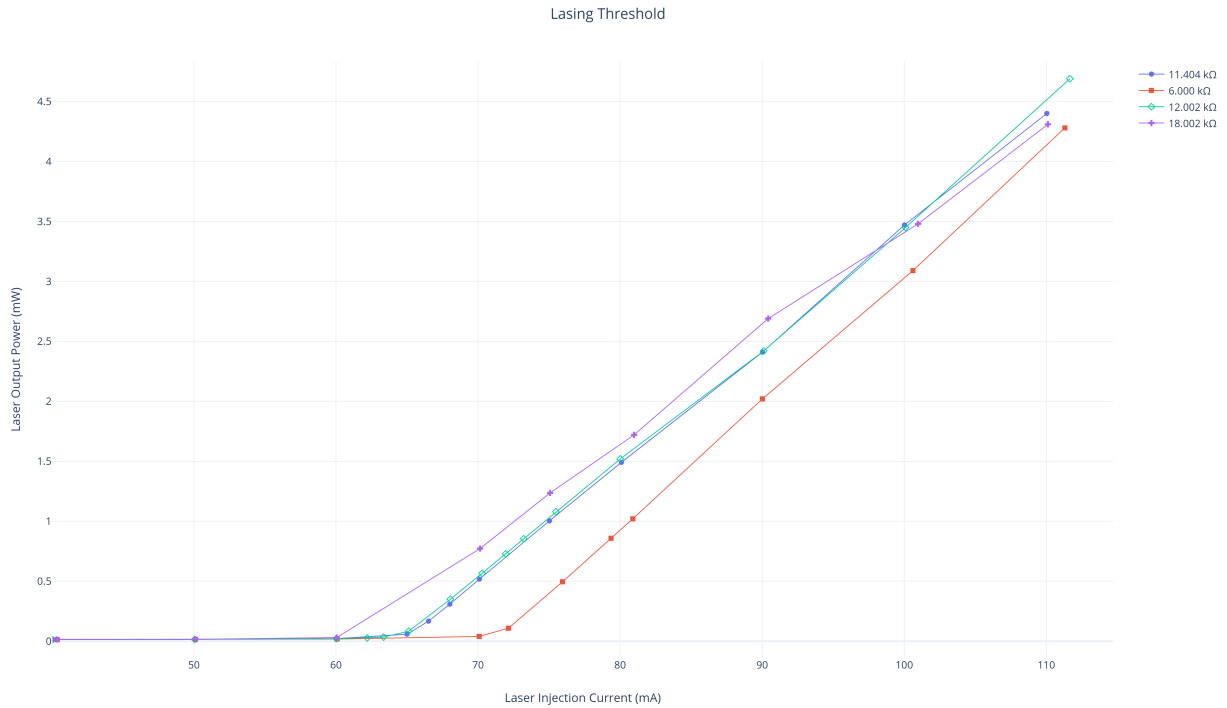
Figure 4.8: Lasing Threshold

and the source. As already mentioned in 2.2.1.1, the output beam was slightly elliptical in shape and suffered from astigmatism. This can be corrected by using cylindrical lenses to rectify the asymmetry of the axes.

It is expected that a collimated laser beam will not have a significant output beam power variance with distance. It is seen in Fig. 4.10 that there is not a very high difference in the output beam power of the laser with increasing distance, with a variation of at most 0.5 mW in the case of a cold laser diode at 18 kΩ with a spontaneous emission background, as seen in Fig. 4.9. The difference in the beam power is more marked with temperature as we see the power characteristics of the output beams grouped together when the temperature is the same. We see though that there is a reduction in the power when the laser is at its farthest from the detection point, in comparison to the power when it is nearest.

Presently, I am tweaking the direction of the vertical plane of the diffraction grating in order to self-inject the master diode laser. Self-injecting the laser will enhance desirable optical feedback, and lead to a reduction in the threshold laser injection current. This will be followed by scanning across a range of injection currents and temperatures to lock the
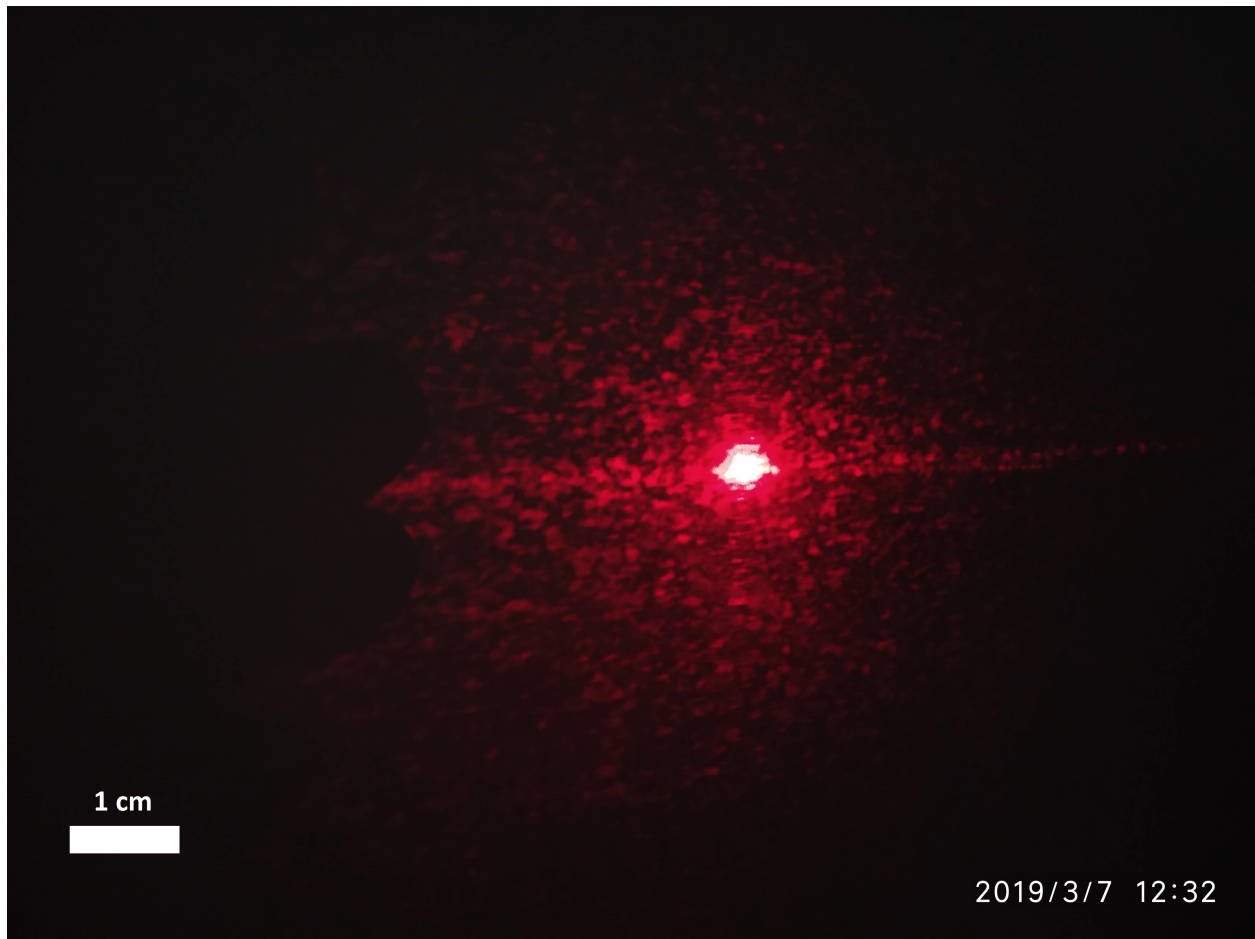
Figure 4.9: Laser Output Beam

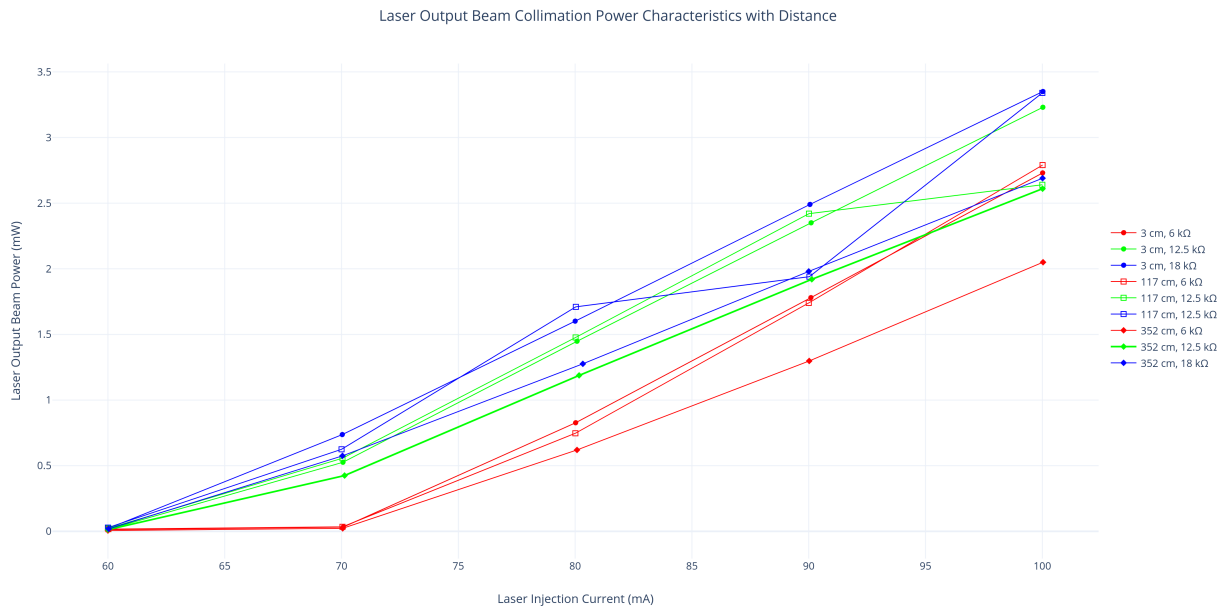wavelength of the master diode laser to a single mode, which in our case is the D1 line of ^{7}Li.

Figure 4.10: Laser Output Beam Collimation Power Characteristics with Distance

Figure 4.11: Complete Experimental Setup (at present)

Chapter 5

Conclusion

In my Masters' project, I have reviewed literature on laser systems and resonators, and understood the basic laboratory techniques in addition to practicing them. Subsequently, I have designed an optical system which should have the desired stability for cooling Lithium atoms in the Lithium 1 lab. I have, till now, worked on constructing the system, and have been able to setup the master diode laser. The initial plan to construct the whole system was decelerated by the problem in stabilizing the temperature of the diode laser, which was a crucial requirement for constructing the whole optical system. I am presently actively working on continuing with the construction of the other parts of the optical system, so that

they can be integrated with the global system in the lab, where experiments with superfluid Lithium will be carried out.

It is instructive to note that understanding the problem with the position of the thermistor was a crucial element in rectifying the seemingly intractable problem of temperature stabilization in the master diode laser of our setup. I would like to point out that this experimental experience and learning has reinforced the ideas of organizing experimental apparatus, exploring and questioning basic elements of the design and keeping track of simple measurements which can help in testing system behaviour and troubleshooting them, when required.

Bibliography

[1] C. De Daniloff, ENS Paris Masters' Thesis, (2018)

[2] S. Tan, Ann. Phys. **323**, pp. 29-52 (2008)

[3] J. T. Stewart *et al.*, Phys. Rev. Lett. **104**, pp. 235-301 (2010)

[4] E. Braaten, In: Zwerger W. (eds) The BCS-BEC Crossover and the Unitary Fermi Gas, Lecture Notes in Physics **836**, Springer (Berlin, Heidelberg), pp. 193-230 (2012)

[5] E. Haller *et al.*, Nat. Phys. **11**, pp. 738-742 (2015)

[6] N. Navon *et al.*, Science **328**, 729 (2010)

[7] K. Dai, EPFL Masters' Thesis, (2018)

[8] S. Giorgini *et al.*, Rev. Mod. Phys. **80**, pp. 12151274 (2008)

[9] H. Kogelnik & T. Li, Appl. Opt. **5**, pp. 1550-1567 (1966)

[10] H. Kogelnik, Appl. Opt. **4**, pp. 1562-1569 (1965)

[11] C.E. Wieman & L. Hollberg, Rev. Sci. Instrum. **62 (1)**, pp. 1-20 (1991)

[12] I. Ferrier-Barbut, ENS Paris PhD Thesis, (2014)

[13] C.J. Sansonetti *et al.*, Phys. Rev. Lett. **107**, 023001 (2011)

[14] R.A. Hyder, ENS Paris Masters' Thesis, (2017)

[15] G. Dash, LKB PhD Presentation, (2018)

[16] J. C. Camparo, Contemp. Phys. **26**, 443 (1985)

[17] J.L. Picque & S. Roizen, Appl. Phys. Lett. **27**, 340 (1975)

[18] M. Arditi & J.L. Picque, Optics Comm. **15**, 317 (1975)

[19] V. Pevtschin & S. Ezekiel, Opt. Lett. **12**, 172 (1987)

[20] P. McNichol & H. J. Metcalf, Anal. Ont. **24**, 2757 (1985)

[21] A. D. Streater, J. Mooibroek, & J. P. Woerdman, Appl. Phys. Lett. **52**, 602 (1988)

[22] R. N. Watts & C. E. Wieman, Opt. Lett. **11**, 291(1986)

[23] C. Salomon *et al.*, Phys. Rev. Lett. **59**, 1659 (1987)

[24] C. E. Tanner *et al.*, Opt. Lett. **13**, 357 (1988)

[25] D. Sesko *et al.*, J. Opt. Sot. Am. B **5**, 1225 (1988)

[26] S. Chu *et al.*, Phys. Rev. Lett. **55**, 48 (1985)

[27] T. W. Hinsch & A. L. Schawlow, Opt. Commun. **13**, 68 (1975)

[28] M.O. Mewes *et al.*, Phys. Rev. A, **61**, 011403(R) (1999)

[29] E. L. Raab *et al.*, Phys. Rev. Lett. **59**, 2631 (1987)

[30] D. Sesko *et al.*, Phys. Rev. Lett. **63**, 961 (1989)

[31] F. Schreck, ENS Paris PhD Thesis, (2002)

[32] L. Ricci *et al.*, Opt. Commun. **117**, 541-549 (1995)

[33] Thorlabs Inc., Operation Manual Version 3.5, Thorlabs Thermoelectric TED200C Temperature Controller, (05 Oct 2017)

[34] Thorlabs Inc., Thorlabs TH10K Thermistor Specifications Sheet, 4813-S01, Rev. D. (19 Oct 2012)

[35] C. Salomon *et al.*, Europhys. Lett., **12**, 683, (1990)

[36] C. Salomon, Cold Atoms, BoseEinstein condensation and Clocks, Lausanne Lectures, (3 April 2014)

[37] N. W. Carlson, Monolithic Diode-Laser Arrays **33**, Springer-Verlag (Berlin, Heidelberg), (1994)

[38] RP Photonics Encyclopedia, Master Oscillator Power Amplifier, URL: [https://www.rp-photonics.com/master_oscillator_power_amplifier.html], (accessed 1 April 2019)

[39] Thorlabs Inc., PID Basics - 12 W Laser Diode Temperature Controllers, URL: [https://www.thorlabs.com/newgrouppage9.cfm?objectgroup_id=307&pn=TED200C], (accessed 1 April 2019)